Coordination of hydraulic thresholds across roots, stems, and leaves of two co-occurring mangrove species

Guo-Feng Jiang[1,2,3]; Su-Yuan Li[1]; Yi-Chan Li[1]; Adam B. Roddy[2,3,4]

[1]Guangxi Key Laboratory of Forest Ecology and Conservation, and State Key Laboratory for Conservation and Utilization of Subtropical Agro-Bioresources, College of Forestry, Guangxi University, Daxuedonglu 100, Nanning, Guangxi 530004, PR China
[2]Author for contact: gfjiang@gxu.edu.cn and aroddy@fiu.edu.
[3]Senior authors
[4] Institute of Environment, Department of Biological Sciences, Florida International University, Miami, FL, USA

Short title: Drought thresholds in roots, stems, and leaves

One-sentence summary

In two mangroves, stomatal closure, turgor loss, and incipient embolism occur over a narrow range of water potentials and result in roots and leaves being more vulnerable to embolism than stems.

The author responsible for distribution of materials integral to the findings presented in this article in accordance with the policy described in the Instructions for Authors (https://academic.oup.com/plphys/pages/General-Instructions) is: Guo-Feng Jiang (gfjiang@gxu.edu.cn) and Adam B. Roddy (aroddy@fiu.edu).

Author Contributions:
G.-F.J. conceived the ideas and designed the study. G.-F.J., S.-Y. Li, Y.-C. Li, and A.B.R. collected the data. G.-F.J. and A.B.R. analyzed the data. G.-F.J. and A.B.R. wrote the manuscript, and all authors reviewed each draft before giving approval for submission of the final version.

ABSTRACT

Mangroves are frequently inundated with saline water and have evolved different anatomical and physiological mechanisms to filter and, in some species, excrete excess salt from the water they take up. Because salts impose osmotic stress, interspecific differences in salt tolerance and salt management strategy may influence physiological responses to drought throughout the entire plant hydraulic pathway, from roots to leaves. Here, we characterized embolism vulnerability simultaneously in leaves, stems, and roots of seedlings of two mangrove species (*Avicennia marina* and *Bruguiera gymnorrhiza*) along with turgor-loss points in roots and leaves and xylem anatomical traits. In both species, the water potentials causing 50% of total embolism were less negative in roots and leaves than they were in stems, but the water potentials causing incipient embolism (5%) were similar in roots, stems, and leaves. Stomatal closure in leaves and turgor loss in both leaves and roots occurred at water potentials only slightly less negative than the water potentials causing 5% of total embolism. Xylem anatomical traits were unrelated to vulnerability to embolism. Vulnerability segmentation may be important in limiting embolism spread into stems from more vulnerable roots and leaves. Interspecific differences in salt tolerance affected hydraulic traits from roots to leaves: the salt-secretor *A. marina* lost turgor at more negative water potentials and had more embolism-resistant xylem than the salt-excluder *B. gymnorrhiza*. Characterizing physiological thresholds of roots may help to explain recent mangrove mortality after drought and extended saltwater inundation.

Keywords: Vulnerability segmentation, embolism resistance, turgor loss, xylem vulnerability curves, mangrove, leaf, stem, root.

INTRODUCTION

Globally forests are threatened by increases in the frequency and severity of droughts, which stress plants beyond their physiological thresholds leading to irreversible hydraulic dysfunction (Choat et al., 2012; Adams et al., 2017; Brodribb et al., 2020a). As plant organs desiccate and their water potentials become more negative, their organs pass a series of thresholds associated with loss of different physiological functions (Bartlett et al., 2016; Trueba et al., 2019; Sorek et al., 2021). Some of these functions, such as declines in leaf gas exchange, are reversible and can recover after short-term droughts, while others, such as the

entry and spread of air embolisms in the xylem are likely irreversible and irreparable, leading to permanent tissue death (Brodribb and Cochard, 2009; Skelton et al., 2017a; Brodersen et al., 2019). How plants survive and recover from droughts depends on the vulnerability of different positions in the transpiration stream from roots to leaves. Indeed, both xylem hydraulic efficiency and the vulnerability of the xylem to air embolism can vary along the hydraulic pathway (Soriano et al. 2020), although rarely have measurements of xylem vulnerability been made in roots, stems, and leaves (Skelton et al., 2017b; Losso et al., 2018; Rodriguez-Dominguez et al., 2018). Furthermore, different plant organs have different construction costs and longevities and may therefore differ in their resistance to embolism. This 'vulnerability segmentation hypothesis' therefore predicts that short-lived, less expensive, and more easily replaceable organs, such as leaves and roots, may be be more vulnerable to embolism than more costly and long-lived structures, such as stems (Zimmermann, 1978; Tyree and Ewers, 1991; Tyree and Zimmermann, 2013). Understanding whole-plant tolerances to prolonged droughts and their potential post-drought recovery depends on quantifying these critical physiological thresholds in response to declining water potentials throughout the entire plant, from the roots to the leaves.

Water moves from the roots to the leaves under tension generated by the evaporation of water inside the leaf and its diffusion from the leaf interior to the atmosphere (Dixon and Joly, 1895). One way of limiting water loss in the face of drought is to close stomata (Jones and Sutherland, 1991; Meinzer, 2002). Stomatal sensitivity to declining water potential can vary among species but is thought to occur prior to incipient xylem embolism (Martin-StPaul et al., 2017; Creek et al., 2020). Because embolism spread through the xylem network is likely irreversible in most species and can lead to mortality, thresholds of embolism resistance–such as the water potentials at stomatal closure, leaf turgor loss, incipient embolism spread (e.g. 5% or 12% of total embolism), and 50% and 88% declines in hydraulic conductivity–are considered key indicators of drought tolerance (Choat et al., 2012; Bartlett et al., 2014; Bartlett et al., 2016; Zhu et al., 2018; Skelton et al., 2018; Skelton et al., 2021). Furthermore, differences in critical water potentials–such as those at which stomatal closure, turgor loss (Ψ_{tlp}), incipient embolism formation (P_5, 5% of total embolism or 5% loss of conductivity), and 50% of total embolism or loss of conductivity (P50) occur–represent safety margins that may themselves indicate different strategies for tolerating or avoiding drought (Choat et al., 2012; Skelton et al., 2018). Understanding the impacts of drought on plant species and their ability to recover after drought requires characterizing these physiological thresholds throughout the entire plant. Yet, rarely have drought thresholds in

leaves, stems, and roots been quantified together.

Quantifying vulnerability to embolism throughout the plant hydraulic pathway and testing the vulnerability segmentation hypothesis have been limited primarily by methodological problems involved in measuring vulnerability to embolism spread in organs more delicate than stems, such as leaves and roots. Traditional hydraulic methods that quantify loss of hydraulic conductivity, though considered the standard to which all other methods are compared, have various artifacts associated with sample preparation (Cochard et al., 2013; Rockwell et al., 2014; Venturas et al., 2019). Until recently, quantifying vulnerability in different organs (e.g., leaves and stems) has required different methods, such as comparing percent loss of hydraulic conductivity of excised stem segments to percent loss of leaf hydraulic conductance. The fragility of some tissues has made them particularly difficult to measure using hydraulic methods (Froux et al., 2005; Johnson et al., 2016). However, recent advances in visualization methods, such as high resolution microcomputed tomography (microCT) and the optical vulnerability (OV) method, have enabled insights into the process of embolism formation (reviewed in Brodersen et al. 2019). Because these visualization methods are often less invasive than hydraulic methods and do not require excision, they have enabled quantification of vulnerability to embolism spread in fragile structures like reproductive organs (Zhang and Brodribb, 2017; Roddy et al., 2018; Bourbia et al., 2020), roots (Rodriguez-Dominguez et al., 2018), and herbaceous leaves (Johnson et al., 2018), as well as higher spatial and temporal resolution of embolism dynamics, such as embolism spread in different leaf vein orders (Brodribb et al., 2016a; Scoffoni et al., 2017) and characterization of changes in tissues other than the xylem during desiccation (Cuneo et al., 2016; Roddy et al., 2018). While these optical methods often produce similar vulnerability curves to those produced by hydraulic methods (Brodribb *et al.*, 2020b; Gauthey et al. 2020), these methods do sometimes disagree, which may be due to a combination of differences in what the methods measure (e.g., declines in hydraulic conductivity versus abundance of embolized vessels) and the influence of xylem network organization and sectoriality on water movement and visualization of embolism (Venturas et al., 2019).

Because these optical methods allow for the same method to be applied to all organs often simultaneously, they enable more direct comparison of vulnerability in different organs. Noninvasive microCT methods have shown leaves to be more vulnerable than stems in *Vitis* species (Charrier et al., 2016), differences in vulnerability among leaves, stems, and roots in *Acer pseudoplatanus* (Losso et al., 2018), differences in vulnerability between leaves and

stems in *B. pendula* and *L. nobilis* (Klepsch et al., 2018), but no vulnerability segmentation in *Fagus sylvatica* (Losso et al., 2018), *L. tulipifera* (Klepsch et al., 2018), and *Pinus pinaster* (Bouche et al., 2016). The optical vulnerability (OV) method has shown roots to be less vulnerable than leaves or stems in olive (Rodriguez-Dominguez et al., 2018), leaves to be more vulnerable than stems in oaks (Skelton et al., 2021) and winter-deciduous woody species (Avila et al. 2021), but no segmentation in tomato (Skelton et al., 2017b) and woody sclerophyllous species (Smith-Martin et al., 2020). This difference in vulnerability between organs within an individual plant may be species-specific and depend on xylem anatomy (Lens et al., 2011; Jansen and Nardini, 2014) and habitat, with species from more arid habitats having greater levels of hydraulic and vulnerability segmentation than those from more mesic habitats (Zanne et al., 2006; Schenk et al., 2008; Zhu et al., 2016).

One particularly interesting group of plants long important in studies of plant hydraulics is mangroves, which are almost constantly exposed to saline water that imposes an energetic demand on water acquisition. Mangroves were the focus of early studies of plant water potential and hydrostatic pressure gradients precisely because extracting water from the soil is more energetically costly in saline than in non-saline soils (Scholander et al., 1962; Scholander et al., 1964; Scholander et al., 1965). Mangroves often rely on highly suberized, hydrophobic bands in the root endodermis called Casparian strips, which help to exclude 85-95% of the salt in their source water from their roots (Krishnamurthy et al., 2014; Reef and Lovelock, 2015). Some species possess glands in their leaves that secrete salt (Waisel et al., 1986), while others lack salt glands but are able to filter out 99% of environmental salt before it enters their roots (Paliyavuth et al., 2004; Reef and Lovelock, 2015). Nonetheless, mangroves typically operate at water potentials substantially more negative than other terrestrial plants due to the very negative osmotic potentials of their saline source water, suggesting that their tissues and organs might be particularly resistant to xylem embolism spread. Yet, relatively little is known about mangrove vulnerability to embolism, with only six true mangrove species having been studied previously. Together, these studies show various degrees of inter- and intra-specific vulnerability to embolism and loss of hydraulic conductivity in stems (Sperry et al., 1988; Melcher et al., 2001; Ewers et al., 2004; Jiang et al., 2017; Jiang et al., 2021a; Jiang et al., 2021b). Notably, in none of these studies has the vulnerability to embolism of either roots or leaves been measured.

In the present study, we quantified differences in vulnerability to embolism among roots, stems, and leaves of seedlings of two common, co-occurring mangrove species: *Avicennia marina* (Forsskål) Vierhapper (Acanthaceae) and *Bruguiera gymnorrhiza* (L.)

Savigny (Rhizophoraceae). Both species are widely distributed across the Indo-West Pacific region and often co-occur, but *A. marina* has greater salinity tolerance and can be found in more extreme habitats (e.g., Red Sea, southern Australia and New Zealand) and low, intermediate, and high intertidal regions, while *B. gymnorrhiza* is moderately tolerant of salt and absent from extreme environments and low intertidal zones (Tomlinson, 1986; Ball, 1988; Clough, 1992; Krauss et al., 2008; Reef and Lovelock, 2015). Differences in habitat preference are associated with differences in salt management strategy: *A. marina* can take up and excrete excess salt, while *B. gymnorrhiza* more effectively excludes salt from the water it absorbs. Because *A. marina* absorbs more salt than *B. gymnorrhiza*, we predicted that *A. marina* would lose physiological functions at more negative water potentials than *B. gymnorrhiza* during drought. Consistent with this hypothesis, these two species exhibit different stomatal and hormonal responses to drought: while *B. gymnorrhiza* rapidly closes its stomata in response to declining leaf water potential and foliar abscisic acid (ABA) accumulation, stomata in *A. marina* are less sensitive to declining leaf water potential and exhibit no response to foliar ABA (Jiang et al., 2021a). We hypothesized (1) that the greater stomatal sensitivity of *B. gymnorrhiza* is associated with greater vulnerability to embolism in roots, stems, and leaves, compared to *A. marina*, which has less sensitive stomata, (2) that leaves would be much more vulnerable to embolism than both stems and roots, (3) that although embolism resistance would differ between species and vary among individuals, embolism resistance would be coordinated among organs *within* individuals, such that, for example, individual plants with more resistant stems would have more resistant roots and leaves, and (4) that stomatal closure would precede turgor loss and incipient embolism spread, resulting in large safety margins between these different drought response thresholds.

RESULTS

Embolism spread in roots, stems, and leaves

Vulnerability curves of the two species were plotted as cumulative embolized area as a function of stem water potential (Fig. 1) to calculate the water potentials at 50% cumulative embolism (P50) and 5% cumulative embolism (P_5), a metric of the water potential at which air first enters the xylem, and additional critical embolism values are reported in Table 1. Consistent with our first hypothesis, *B. gymnorrhiza* was overall more vulnerable to embolism than *A. marina*, though the differences between species were less apparent when comparing the P_5 values than when comparing the P50 values (Fig. 1 and Fig. 2, Table 1).

Species (df = 1, F = 16.47, P < 0.01) but not organs differed significantly (df = 1, F = 2.04, P = 0.20) in the P_5. Similarly, species (df = 1, F = 37.63, P < 0.001) but not organs (df = 1, F = 0.92, P = 0.37) differed significantly in the P50.

In contrast to our second hypothesis, roots were the most vulnerable organ in both species, although root vulnerability did not differ significantly from that of leaves (Fig. 1 and Fig. 2, Table 1). To characterize differences among organs in the P_5 and P50 for each species separately, we used linear mixed effects models that included a random effect of individual plant to account for the fact that organs were measured on the same individual plants (Fig. 2). In *A. marina*, the P_5 did not differ significantly between organs, while in *B. gymnorrhiza* the P_5 did differ significantly between stems and roots (z = 3.99, P < 0.001), but not between leaves and either stems (P = 0.14) or roots (P = 0.20) (Fig. 2a). In *A. marina*, the P50 differed significantly between stems and roots (z = 9.85, P < 0.001), between stems and leaves (z = 7.04, P < 0.001), and between roots and leaves (z = 2.81, P < 0.05) (Fig. 2b). In *B. gymnorrhiza*, the P50 differed significantly between stems and both roots (z = 5.54, P < 0.0001) and leaves (z = 3.89, P < 0.001) but not between roots and leaves (P = 0.51) (Fig. 2b). To compare these values of P50 obtained using the optical methods to those obtained using traditional hydraulic methods, we also compiled previously reported P50 values for various mangrove species (Fig. 2b). Data from previous studies come entirely from mature adults measured using hydraulic methods and report only the P50 values. These previous data show substantial intraspecific variability in P50: P50s of *Avicennia marina* and *Aegiceras corniculatum* vary by 2.7 and 3.0 MPa, respectively, across three sites in Australia (Jiang et al., 2021b), and the P50 of *Rhizophora mangle* varies by 2.0 MPa between nearby coastal and estuarine sites (Melcher et al., 2001).

We also tested whether there was coordination in embolism resistance among organs within individual plants. Within individuals, both *A. marina* and *B. gymnorrhiza* showed the same trend in embolism resistance across organs (from least resistant to most resistant) within individual plants: roots < leaves < stems (Fig. 3), although differences in P50 between roots and leaves were not significant in *B. gymnorrhiza* (LME; P > 0.05). Within individual plants, both the P_5 (df = 2, F = 8.64, P < 0.01) and the P50 (df = 2, F = 34.78, P < 0.0001) differed significantly among organs. Despite these significant differences in the P50 between organs within individuals, there was little evidence that plants with more vulnerable xylem in one organ also had more vulnerable xylem in other organs (Fig. 4). While there were significant pairwise correlations between organ P50s among individual plants, these were driven predominantly by the large differences in P50 between species across all organs (Fig. 4).

Within species, the P50s of only roots and leaves were significantly correlated with each other, and this coordination between root P50 and leaf P50 was very strong and highly significant within each species (*A. marina*: $r^2 = 0.99$, $P < 0.0001$; *B. gymnorrhiza*: $r^2 = 0.99$, $P < 0.01$; Fig. 4b). Thus, in contrast to our third hypothesis, individual plants with more vulnerable stems did not necessarily have more vulnerable leaves or roots (Fig. 4a, c).

Safety margins between stomatal closure, turgor loss, and incipient embolism

We further compared these xylem vulnerability curves to measurements of stomatal conductance (g_s) as a function of leaf water potential and the water potential at turgor loss (Ψ_{tlp}) in order to determine the order of physiological responses to declining water potential and to assess hydraulic safety margins. We used recently published measurements of stomatal conductance measured during a drought experiment on individuals of similar age and size from both species (Jiang et al. 2021a). Integrating the response of g_s to drought with our measurements of vulnerability to embolism showed that while g_s of *B. gymnorrhiza* was more sensitive to declining water potentials than g_s of *A. marina* (blue lines in Fig. 1; Jiang et al., 2021a), in both species complete stomatal closure occurred at similar water potentials as both turgor loss and the P_5 (Table 1; Fig. 1; Table 2 in Jiang et al., 2021a). In both species, the water potential at stomatal closure (i.e., g_s at 5% of its maximum) was only slightly less negative than the leaf P_5. In *A. marina* stomatal closure occurred at the same water potential as leaf turgor loss, while in *B. gymnorrhiza* stomatal closure was slightly more negative than the Ψ_{tlp}, in contrast to our fourth hypothesis.

Contrary to our fourth hypothesis that there would be large safety margins between turgor loss and incipient embolism spread, we found that across both roots and leaves, turgor loss generally occurred at only slightly higher water potentials than the P_5, indicative of narrow safety margins between turgor loss and incipient embolism spread (Fig. 5, Table 1). The largest safety margin between Ψ_{tlp} and P_5 was 1.55 MPa, which occurred for *A. marina* roots (Fig. 5, Table 1). All other safety margins between turgor loss and incipient embolism were less than 0.7 MPa, with the narrowest (0.26 MPa) occurring in *B. gymnorrhiza* roots.

Xylem vulnerability to embolism and xylem anatomy

A. marina had smaller diameter xylem vessels than *B. gymnorrhiza* ($df = 1$, $F = 335.96$, $P < 0.001$) (Fig. 6). Vessel diameters differed among organs ($df = 2$, $F = 946.07$, $P < 0.001$), and

these differences among organs were species-dependent (i.e., there was a significant species x organ interaction; df = 2, F = 49.83, P < 0.001). For *A. marina*, there was no significant difference between stem and root vessel diameters (P = 0.44), but leaf vessel diameters were significantly smaller than both stem (z = 22.09, P < 0.001) and root (z = 15.36, P < 0.001) vessel diameters. For *B. gymnorrhiza*, vessel diameters were progressively smaller moving from the roots to the leaves, with leaves having smaller vessels than both stems (z = 22.40, P < 0.001) and roots (z = 30.80, P < 0.001) and stems having smaller vessels than roots (z = 11.56, P < 0.001). There were no significant linear relationships between any xylem anatomical traits and either P50 or P_5 across organs or species (all P > 0.05; Fig. 7).

DISCUSSION

Mangroves have long been important in the study of plant water relations (Scholander et al., 1962; Scholander et al., 1964; Scholander et al., 1965). Despite having constant access to water, mangroves are exposed to near constant osmotic stress because this environmental water is saline. To create sufficient tension to drive water uptake, mangroves must reduce the osmotic potential in their cytoplasm by accumulating solutes (Reef and Lovelock, 2015), resulting in more negative turgor loss points (Ψ_{tlp}) that can vary with growth salinity (Paliyavuth et al., 2004; Nguyen et al., 2017). Because stomatal closure and turgor loss are thought to occur at less negative water potentials than those at which air embolisms in the xylem form and spread (Skelton et al., 2018; Trueba et al., 2019; Bourbia et al., 2020; Creek et al., 2020; Dayer et al. 2020), we predicted that interspecific differences in salt tolerance would be associated with differences in drought response thresholds throughout the entire plant hydraulic pathway. Here, we characterized embolism formation and spread simultaneously in roots, stems, and leaves of seedlings of two common mangrove species, in combination with measurements of stomatal responses to declining leaf water potential and leaf and root turgor loss points. As we predicted, (1) there were large interspecific differences in vulnerability between these two co-occurring mangrove species that differ in salt tolerance, (2) although stems were more resistant to embolism than both leaves and roots, as we had predicted, roots were surprisingly vulnerable to embolism, and (3) there was coordination in vulnerability across organs within individuals but only for roots and leaves. However, in contrast to our predictions, (4) safety margins between stomatal closure, turgor loss, and incipient embolism spread were very narrow. These results suggest that the saline environment has coordinated effects on cell water balance, stomatal responses, and xylem vulnerability throughout the entire hydraulic pathway from roots to leaves in mangroves.

Quantifying embolism thresholds simultaneously in multiple organs on individual plants allows a more complete characterization of thresholds of drought responses, particularly in combination with other physiological measurements (Skelton et al., 2018; Rodriguez-Dominguez et al., 2018; Smith-Martin et al., 2020; Bourbia et al., 2020; Avila et al., 2021). Because stomatal closure limits water loss that can result in xylem embolism, we predicted that species with greater stomatal sensitivity to declining water potential may also have xylem more vulnerable to embolism. Previous work on seedlings of these two mangrove species has shown that stomatal conductance is more than twice as sensitive to declining leaf water potential in *B. gymnorrhiza* than it is in *A. marina*, and this greater sensitivity of g_s in

311 *B. gymnorrhiza* is associated with a strong ABA response that is absent in *A. marina* (Fig. 1;
312 Jiang et al., 2021a). Thus, the greater stomatal control in *B. gymnorrhiza* may protect its more
313 vulnerable xylem (Fig. 1 and Fig. 2).

314 In addition to overall differences in vulnerability between the two species, in both *A.*
315 *marina* and *B. gymnorrhiza* roots and leaves were more vulnerable to embolism than stems,
316 consistent with the vulnerability segmentation hypothesis (Fig. 1 and Fig. 2; Zimmermann,
317 1978; Tyree and Zimmermann, 2013). Our finding that roots of both *A. marina* and *B.*
318 *gymnorrhiza* were at least as vulnerable as leaves and significantly more vulnerable than
319 stems (Fig. 2) was surprising and suggests that embolism resistance does not vary
320 monotonically along the transpiration stream from the roots to the leaves, as has been shown
321 for *Olea europaea* (Rodriguez-Dominguez et al., 2018). Because there are many leaves and
322 roots attached to the stem, any single root or leaf may not need to maintain high embolism
323 resistance. This could explain why there is variation in embolism vulnerability between
324 individual roots or leaves on the same plant (Cardoso et al. 2020). The lack of structural
325 redundancy in the stem, which integrates the water taken up by all the roots and distributes it
326 to the leaves, may require it to be more resistant to embolism formation than roots or leaves.
327 Indeed, in habitats where the risk of hydraulic failure is greater, stems are often more
328 segmented and less hydraulically integrated in order to increase hydraulic redundancy (Zanne
329 et al., 2006; Schenk et al., 2008). The ability to absorb water through shoots and leaves may
330 alleviate selection for embolism-resistant roots by providing an alternative pathway for water
331 entry, which may be particularly beneficial to mangroves because root-available water is so
332 often saline (Fuenzalida et al., 2019; Schreel et al., 2019). If building more embolism-
333 resistant roots is costly, then having roots so vulnerable to turgor loss and embolism could
334 restrict mangroves to living where freshwater is readily available. Thus, interspecific
335 differences in root vulnerability may partially explain the fine-scale niche differences
336 between these two species: *B. gymnorrhiza* is excluded from low intertidal zones and often
337 occurs near brackish water, while *A. marina* occurs in more extreme habitats and at all
338 intertidal zones (Tomlinson, 1986; Ball, 1988; Clough, 1992).

339 Despite the large variation in vulnerability among species and organs, there was little
340 evidence for coordination in vulnerability across organs within individual plants, and
341 variation in vulnerability was unrelated to the anatomical traits we measured. Only root P50
342 and leaf P50 were coordinated within species (Fig. 4b), and P50s of no other organ pairs were
343 similarly coordinated within species, in contrast to results for *Olea europaea* (Rodriguez-
344 Dominguez et al., 2018). The large variation in embolism vulnerability observed among

345 species and organs was unrelated to any xylem anatomical trait measured here (Fig. 7): leaves
346 had significantly narrower vessels than stems and roots (Fig. 6; Table 1), but leaves were no
347 more resistant to embolism than stems or roots (Fig. 2). We also compared our data for
348 mangroves to data from recently published studies in order to identify whether mangroves
349 may be uniquely different in their anatomical traits and embolism vulnerability. The bivariate
350 distributions of P50s and anatomical traits of these two mangroves were similar to those of
351 six other species (Fig. 7). We extend these analyses to show that these anatomical traits also
352 do not correlate with the P_5. Although these anatomical traits have been considered important
353 predictors of P50 (Hacke et al., 2001; Brodribb & Holbrook, 2005; Jiang et al., 2017; Olson
354 et al., 2018; Liu et al., 2019; Degraeve et al., 2021; Thonglim et al., 2021), our results and
355 other recent studies have found no relationships between xylem P50s and these anatomical
356 traits (Rodriguez-Dominguez et al., 2018; Losso et al., 2018; Avila et al., 2021).
357 If embolism vulnerability depends on air entry into the xylem, then traits other than
358 the xylem anatomical traits we measured may be more predictive of xylem vulnerability to
359 embolism. These may include the wettability of the xylem, the location of air around the
360 xylem, proximity to already embolized conduits, and the location and structure of pits where
361 air can seed into the xylem (Lens et al., 2011; Guan et al., 2021; Kaack et al., 2021).
362 Additionally, these traits may have different effects on initial air entry (e.g., the P_5) and later
363 embolism spread (e.g., the P50). Only the more vulnerable *B. gymnorrhiza* exhibited
364 significant differences among organs in initial air entry thresholds (Fig. 2). The more
365 embolism-resistant *A. marina* had statistically indistinguishable P_5 values in roots, stems, and
366 leaves, suggesting that xylem in these organs is equally vulnerable to initial air entry.
367 However, significant differences in P50s among *A. marina* organs suggest that organs
368 differed in the rate at which air embolism spreads once it is present in the xylem network,
369 with stems having more gradual accumulation of embolized vessel area compared to leaves
370 and roots (Fig. 3). Embolism spread through the xylem network depends on having a source
371 for the gas that fills conduits, and already embolized conduits can provide a source and
372 pathway for air to seed from one vessel to another (Guan et al., 2021). Other xylem traits
373 besides those measured here, such as conduit end walls and their pit membranes, have been
374 suggested to influence how readily air embolisms move from conduit to conduit, and
375 differences in these traits among organs could explain the inter-organ differences in
376 embolism accumulation that we observed (Figs. 1-3; Zhang et al., 2017; Kaack et al., 2019;
377 Zhang et al., 2020; Guan et al., 2021). Air can also be present in other parts of the plant
378 besides embolized conduits, such as the leaf mesophyll or aerenchyma in stems and roots.

Because they almost always stand in water, mangroves often produce aerial roots with lenticels that allow for air entry into the roots and distribution through aerenchyma (Purnobasuki & Suzuki, 2005). The location of aerenchyma in the roots relative to the xylem may be important in determining vulnerability to initial air entry (i.e., P_5). Integrating other methods for characterizing embolism spread, such as the pneumatic method, and characterization of other traits, such as the spatial distribution of aerenchyma and pit structure, may improve our understanding of the relationship between xylem structure and embolism vulnerability (Guan et al., 2021).

Because mangroves are often exposed to saline water and because increasing salinity can result in more negative Ψ_{tlp} (Nguyen et al., 2017), we predicted that interspecific differences in salinity tolerance may have cascading consequences on multiple physiological thresholds throughout the plant and impact hydraulic safety margins (Fig. 8). As drought proceeds, it is thought that stomatal closure occurs as positive turgor pressure is lost, which is then followed by embolism formation and spread through the xylem (Jones and Sutherland, 1991; Bartlett et al., 2016; Skelton et al., 2018; Trueba et al., 2019; Sorek et al., 2021). Maintaining positive turgor pressure is required for stomata to remain open, and so it is perhaps not surprising that Ψ_{tlp} and g_s closure occurred at similar water potentials in the mangroves studied here (Table 1, Fig. 1). After turgor loss, embolisms can appear in the xylem, and leaves of some species exhibit large safety margins between turgor loss and incipient embolism spread (Dayer et al., 2020; Avila et al., 2021; Sorek et al., 2021). However, we found relatively narrow safety margins between turgor loss and the P_5, though they were not as narrow as has been reported for oak leaves (Skelton et al., 2018). Because turgor loss involves plasmolysis (Scholander et al., 1964) and, in some organs, tissue collapse (Roddy et al., 2018), turgor loss may cause irreversible tissue changes that may do little to forestall embolism formation in the xylem (Cuneo et al., 2016). While the order of these key physiological thresholds within organs did not differ substantially from other species (Bartlett et al., 2016; Trueba et al., 2019), the range of water potentials over which many of these physiological changes occurred in these two mangroves was remarkably small and they occurred at less negative water potentials than expected (Fig. 8). Because growth salinity can alter Ψ_{tlp} (Nguyen et al., 2017) and may also affect embolism vulnerability (Melcher et al., 2001; Jiang et al. 2021b), environmental salinity may drive plasticity in multiple hydraulic traits throughout the plant. We also found that more osmotically active solutes in leaves and roots was associated with more negative P50 (Fig. S4), further suggesting that exposure to saline water may drive shifts in vulnerability to embolism.

Given that mangroves are almost constantly inundated with saline water, we had predicted that they would have xylem very resistant to embolism. Yet roots were as vulnerable to embolism as leaves (Fig. 8, Table 1), suggesting that changes in root hydraulics may be mechanistically linked to stomatal closure (Abdalla et al. 2022) and overall drought tolerance (Bartlett et al. 2022). The narrow range of these critical physiological thresholds suggests that mangroves may be very sensitive to small changes in their environment, such as unusually long saltwater inundation due to extreme weather events (Lagomasino et al. 2021), prolonged drought that precludes freshwater inputs (Duke et al., 2017; Mafigholami et al., 2017), or other stresses that would inhibit their ability to filter out or excrete salts. Thus, better characterizing critical physiological thresholds, particularly in roots, may provide critical mechanisms useful in modeling species responses to a changing climate and extreme weather events.

CONCLUSIONS

Mangroves have long been of interest because of the unique challenges imposed by being nearly constantly inundated with saline water. Here we show that the mangroves studied here experienced stomatal closure, turgor loss, and embolism formation over a very narrow range of water potentials that was not substantially different from those reported for other terrestrial species. Mangrove leaves and roots were equally vulnerable to embolism and more vulnerable than stems, despite the fact that roots are often constantly inundated with saline water and often experience more negative water potentials than many other terrestrial plant species. The structural and physiological adaptations that allow mangroves to exclude most environmental salt from the water they absorb may relax selection for particularly negative turgor loss points or embolism-resistant xylem. Differences between these two species in salt management strategy may be responsible for interspecific differences in these drought thresholds, suggesting that differences in salt tolerance may influence physiological thresholds from roots to leaves.

Our results also highlight how characterizing physiological responses to drought throughout the entire plant hydraulic pathway can provide explanations for observed ecological phenomena. Mangroves globally are threatened by climate change-induced drought and extreme saltwater inundation, both of which have caused large-scale mangrove mortality (Duke et al., 2017; Mafigholami et al., 2017; Saintilan et al., 2020; Lagomasino et al. 2021). Despite living in environments characterized by more negative water potentials

than are experienced by many other terrestrial plant species, mangroves are surprisingly vulnerable to conditions that induce water potential declines. Characterizing these drought thresholds in more mangrove species from different habitats will be critical in predicting mangrove responses to future climate change and to maintaining mangrove forests.

MATERIALS AND METHODS

Plant species and study site

Seedlings of *Avicennia marina* and *Bruguiera gymnorrhiza* were initially grown on the beach at the Guangxi Mangrove Research Center, Guangxi Academy of Sciences, Guangxi, China, in 10 cm x 10 cm square pots that were 20 cm high and filled with seashore soil substrate from the adjacent mangrove forest (Fig. S1). The pots were partially sunk into the soil so that the soil level inside the pots was only about 5 cm above the soil level outside the pots. The seedlings were grown under full sun and exposed to natural tide inundation. When seedlings were approximately two years old and about 50-70 cm height above the soil surface, pots were extracted from the soil, keeping the root system intact in the pots, and transported to Guangxi University, Nanning (Guangxi, China), where they were grown in a glasshouse with natural lighting (full-sun except for partial shading by the glasshouse itself) and natural variability in temperature (15-35 ℃) and air humidity (60-90%). For the 1-3 months until measurements commenced, pots were kept in secondary buckets filled with water and salt (NaCl, 0.6% w/v in water). The water level in the secondary buckets was maintained by refilling with tap water to just above the soil surface 1-2 times per week. During this time, a slow-release fertilizer was applied once every two weeks.

Optical vulnerability (OV) curves

The vulnerability of roots, stems, and leaves to embolism spread was quantified simultaneously on individual plants using the optical method, according to the description of Brodribb *et al.* (2016; 2017). Images were captured using custom-built OpenSourceOV (OSOV; http://www.opensourceov.org) clamps with 20x magnification hand lenses for stems and 40x magnification hand lenses for leaves and roots, following the instructions at http://www.opensourceov.org. Images were captured every 5 min using reflected light for stems and roots of both species and for leaf midribs of *B. gymnorrhiza* and using transmitted light for leaves of *A. marina*. Images were collected until no more changes in observed

reflectance or transmittance were observed for 24 hours, which took a total of approximately 145 hours for each species. All image sequences were analyzed according to the instructions at http://www.opensourceov.org using Fiji (Schindelin et al., 2012). Embolism events in the xylem are notable because they are spatially large and produce intense color changes between sequential frames. During desiccation other tissues can change color, but these color changes are more gradual (i.e., lower intensity) and are smaller in size.

We sampled five seedlings of *A. marina* and four seedlings of *B. gymnorrhiza*. We chose seedlings whose main stems measured 50-70 cm in length for OV imaging. At their bases, stem diameters were approximately 10 mm, and close to their apical tips stem diameters were approximately 2-6 mm. For measurements of stems, a small area of the bark about 20-30 mm in length was carefully removed to expose undamaged xylem from one side of the stem, and a thin layer of hydrogel (Tensive Gel; Parker Laboratories Inc., Fairfield, NJ, USA) was applied immediately to the exposed stem to prevent desiccation during image capture. For measurements of roots, the seedlings were gently extracted from the potting medium by first removing the pot and gently rinsing the soil with water to wash it away and expose the roots, which were wrapped in wet paper towel during installation of the OSOV clamp on stems and leaves. The main roots, which measured 2-5 mm in diameter, were chosen for vulnerability measurement and a small area of the bark about 20-30 mm in length was carefully removed to expose undamaged xylem from one side of the root, where a thin layer of hydrogel was applied to prevent desiccation. For measurements on leaves, mature leaves from current year branches were chosen. Leaf veins of *A. marina* were easy to visualize using transmitted light, but the leaves of *B. gymnorrhiza* were too thick to be visualized using transmitted light. Instead, leaf midribs of *B. gymnorrhiza* were visualized with reflected light, as has been done on leaves of other species (Rodriguez-Dominguez *et al.*, 2018). Visualizing *B. gymnorrhiza* leaf midribs required that some epidermal tissue surrounding the midrib was removed. To determine how much tissue could be removed without damaging the xylem, we first made cross-sections of the midribs of several leaves to determine the depth of the xylem in the midrib. To prevent desiccation during measurements due to removing the epidermal tissue, the exposed midrib was covered with hydrogel. After vulnerability measurements, imaged regions of roots, stems, and leaves were excised and cross-sections made primarily to measure vessel anatomical traits (described below) but also to check whether tissue removal during OV clamp installation damaged the xylem. We found no evidence from these cross-sections that too much tissue had been removed, consistent with other reports that careful sample preparation does not embolize the xylem

513 (Johnson et al., 2020).

514 Stem water potential was monitored simultaneously with embolism visualization
515 using a stem psychrometer (model PSY1; ICT, Australia). The psychrometer was installed on
516 each measured stem close to the base where the diameter was approximately 10 mm, and at
517 about 20 cm proximal to the stem region being imaged. We installed the stem psychrometer
518 on the thickest region of the stem. Water potential was recorded every 10 min, while the
519 cooling time for the psychrometer was checked to ensure precise measurement of the wet-
520 bulb temperature. To further validate the psychrometer measurements after installation, we
521 made periodic (4-6 times within the first 48 h) measurements of leaf water potential using a
522 Scholander pressure chamber (0.01 MPa resolution; PMS Instrument Company, Albany, OR,
523 USA) (Fig. S2). If the psychrometer and pressure chamber were in good agreement in the
524 first 48 h, we stopped measuring leaves with the pressure chamber to prevent removing too
525 many leaves. For plants on which psychrometer measurements could not be made, we
526 periodically measured the potentials of leaves covered with aluminum foil and bagged so that
527 they could equilibrate with stem water potential. These measurements on leaves were spaced
528 to encompass the duration of the optical embolism events. To match water potential to
529 embolism events, we assumed water potential declined linearly between consecutive water
530 potential measurements, allowing interpolation of water potential at every time point. During
531 OV measurements, plants were kept in a small laboratory where the temperature was held
532 constant and where the windows were covered and the lights kept off in order to allow the
533 plants to slowly desiccate and water potentials to equilibrate.
534

535 ## Xylem anatomy

536 After samples were removed from the OV clamps, the imaged regions of roots, stems, and
537 leaf petioles were excised and stored in FAA solution (Formaldehyde, 5% v/v; Acetic acid,
538 5% v/v; Ethyl alcohol, 55% v/v; Water, 35% v/v) until being sectioned using a Leica
539 microtome (Model RM 2235, Leica Microsystems). Cross-sections were stained with 1%
540 (w/v in water) Alcian blue solution for 1-5 min, then washed with water and stained with
541 Safranin O (0.5% w/v in water) for 15 min, to increase visual contrast and imaged at 20x
542 magnification on a Leica DM3000 microscope fitted with a DFC295 CCD camera using LAS
543 software (Leica Microsystems, Wetzler, Germany). Vessels were measured in Fiji
544 (Schindelin et al., 2012) by measuring two perpendicular diameters of each lumen and the
545 thickness of the double wall (*t*) between two adjacent lumens. Because small vessels are

546 unlikely to be observed by the optical devices and because small vessels contribute very little
547 to water flow, we measured only vessels with lumen diameters > 5 μm. In roots and stems,
548 we found no vessels smaller than even 10 μm in diameter. Vessel diameter (*b*) was
549 calculated from these two perpendicular diameters by assuming that lumens were ellipses in
550 cross-section, which was then used to calculate the diameter of a circle with an equivalent
551 area. The thickness to span ratio, $(t/b)^3$, is often considered a measure of resistance to conduit
552 collapse and, therefore, is thought to be linked to vulnerability to embolism (Hacke et al.,
553 2001; Brodribb and Holbrook, 2005). Although we did not measure the distance from the
554 apex where anatomical traits were sampled, these measurements were made on the same
555 region of each organ that was visualized for embolism vulnerability measurements.
556

557 ## Measurement of pressure–volume curves

558 Pressure-volume curves were constructed for leaves (n = 3) and roots (n = 3) of both species,
559 following protocols published for leaves and other organs (Tyree and Hammel, 1972; Nguyen
560 et al., 2017; Roddy et al., 2019) and briefly described here. Seedlings from the greenhouse
561 were moved to the laboratory, then watered and covered with a black plastic bag overnight to
562 allow rehydration prior to leaf and root excision for pressure-volume curve measurements.
563 Root samples about 4-6 cm in length and 2-4 mm in width were carefully cut from the
564 seedlings, gently washed of soil, blotted dry with paper towels, and their water potential and
565 root mass measured sequentially, using the same procedure as is typical for leaf pressure-
566 volume curves. Initial water potentials of roots and leaves were between -1.0 to -2.0 MPa for
567 both species. In mangroves, water potentials close to zero are typically thought to be driven
568 by the presence of large amounts of extracellular water, such that estimates of water potential
569 and relative water content at full turgor are typically lower, near -1.0 MPa (Nguyen et al.,
570 2016). How negative mangrove leaf water potentials and turgor loss points are can depend on
571 both salt management strategy and environmental salinity (Nguyen et al., 2017; Jiang et al.,
572 2017). Pressure-volume curves were constructed by repeatedly measuring the bulk leaf or
573 root water potential using a pressure chamber and subsequently the fresh mass on a balance
574 (resolution of 0.0001 g; Mettler - Toledo Ltd., Greifensee, Switzerland). The pressure
575 chamber was kept humidified with wet paper towels to prevent evaporation from the sample
576 during the water potential measurement. Three samples were measured for each structure of
577 each species, and the three replicates were sampled from different individual seedlings.
578 Between consecutive measurements, specimens were briefly exposed to ambient laboratory

air and then enclosed in humidified plastic bags for approximately 20 min to allow equilibration of water potentials, and time intervals between measurements were lengthened when specimens reached the point of turgor loss. After the conclusion of the measurements, leaf and root samples were oven-dried at 70°C for at least 72 h before determining dry mass that was then used in subsequent calculations. The relationship between water potential and water content was determined for each sample and parameters estimated from pressure-volume curves derived using standard methods (Sack and Pasquet-Kok, 2011).

Data analysis

All statistical analyses were conducted using R software (version 3.4.4, R Development Core Team, Vienna, Austria). Cumulative pixel area of embolized vessels was plotted against the corresponding water potential in order to quantify critical percent embolism values (5% and 50% of total cumulative embolism) for each sample. We extracted the water potentials for each sample at these critical embolism values directly from the curves. For comparison, we also used the 'fitplc' R package to estimate these water potentials at critical embolism values, using both the Weibull and sigmoidal curve fits and compared these to the water potentials extracted directly from the curves. Overall, there was strong agreement across the three sets of estimates for the critical water potential values (Fig. S3). We compared differences between species and organs in the P50 and P_5 using ANOVA and, because all three organs were measured concurrently on the same individuals, an error term for the individual plant. ANOVA results were consistent with results from linear mixed effects (LME) models computed using the R package 'lme4' (Bates et al., 2014). Based on these results, we analyzed species separately to identify the differences between organs, and because pairwise post-hoc comparison in models with random effects cannot be performed using ANOVA, we computed post-hoc comparisons only for linear mixed effects using the R package 'multcomp' (Hothorn et al., 2008). Like the ANOVAs, these linear mixed effects models included an interaction between the fixed effects of species and organ and a random effect of individual plant. We also compared our measurements of optical P50 to previously published P50 values measured using hydraulic methods for mangroves in order to better contextualize our measurements.

Supplemental Data

Supplemental Figure S1. Initial germination and growth conditions of seedlings at the Guangxi Mangrove Research Center.

Supplemental Figure S2. Relationships between water potentials (measured by psychrometer and pressure bomb) and time for three exemplary plants.

Supplemental Figure S3. Relationship between water potentials at critical embolism values estimated by curve fitting using the R package 'fitplc' and measured directly from optical vulnerability curves.

Supplemental Figure S4. Relationships between critical optical embolism values and the number of moles of solutes per root or leaf dry mass.

Funding information

This work was supported by a research grant from the Natural Science Foundation of China (31860195) to G.-F.J.

ACKNOWLEDGMENTS

We thank Dr. Zhi-Nan Su from Guangxi Mangrove Research Center, Guangxi Academy of Sciences for providing seedlings. Three anonymous reviewers and the editor provided valuable and constructive feedback that greatly improved this manuscript. This is contribution #1447 from the Institute of Environment at Florida International University.

630 **Tables**

631 **Table 1**. Comparison of anatomical, pressure-volume, xylem vulnerability, and stomatal
632 conductance traits for roots, stems, and leaves of *A. marina* and *B. gymnorrhiza* seedlings.
633 Values represent means ± standard errors for each organ and species (n = 4-5 for embolism
634 vulnerability; n = 3 per organ per species for turgor loss and for xylem anatomy); . Stomatal
635 conductance (g_s) data are taken from Jiang et al. (2021a) and was measured during a drought
636 experiment of similarly aged and sized individuals of the same species and populations
637 measured here. Water potentials at which 5% (P_5), 12% (P_{12}), 50% (P50), and 88% (P_{88}) of
638 total embolism occurred are reported for each organs. For roots and leaves, the water
639 potential causing turgor loss (Ψ_{tlp}) is reported and is based on pressure-volume curves. See
640 text for statistical comparisons.

Species	Organ	P_5 (MPa)	P_{12} (MPa)	P50 (MPa)	P_{88} (MPa)	Ψ_{tlp} (MPa)	Ψ at 5% of maximum measured g_s (MPa)	Vessel diameter (μm)	Double-wall thickness (μm)
A. marina	leaf	-4.91 ± 0.33	-5.12 ± 0.32	-6.12 ± 0.34	-7.37 ±0.43	-4.36 ± 0.07	-4.35	13.38 ± 0.30	2.28 ± 0.15
	stem	-5.30 ± 0.46	-5.86 ± 0.59	-8.10 ± 0.34	-10.65 ± 0.74	NA	NA	23.17 ± 1.68	2.77 ± 0.35
	root	-4.37 ± 0.35	-4.45 ± 0.38	-5.33 ± 0.40	-9.32 ± 1.10	-2.82 ± 0.13	NA	24.82 ± 2.24	2.61 ± 0.15
B. gymnorrhiza	leaf	-3.38 ± 0.20	-3.44 ± 0.25	-3.87 ± 0.19	-4.37 ± 0.22	-2.68 ± 0.21	-3.25	17.13 ± 1.21	2.36 ± 0.21
	stem	-3.85 ± 0.42	-4.15 ± 0.38	-4.69 ± 0.26	-5.18 ± 0.20	NA	NA	30.16 ± 0.19	2.92 ± 0.13
	root	-2.58 ± 0.28	-2.69 ± 0.31	-3.42 ± 0.26	-3.78 ± 0.15	-2.32 ± 0.36	NA	38.78 ± 1.09	3.16 ± 0.34

641

642

643

FIGURE LEGENDS

Fig. 1 The coordination between optical vulnerability, stomatal closure, and turgor loss as a function of stem water potential for two mangrove species. Optical vulnerability curves of (a) leaf, (b) stem, and (c) root of *Avicennia marina* (green lines, n = 5 seedlings), and (d) leaf, (e) stem, and (f) root of *Bruguiera gymnorrhiza* (purple lines, n = 4 seedlings). The mean water potential causing incipient (5%) of total embolism (P_5) ± s.e. (inverted black triangles and error bars) and the mean water potential causing 50% of total embolism (P50) ± s.e. (black circles and error bars) are plotted for each species x organ group. The stomatal conductance (g_s) as a function of leaf water potential for each species (blue lines; Jiang et al., 2021a) is plotted in (a) and (d). The mean water potentials at turgor loss (Ψ_{tlp}) ± s.e. (dashed lines and grey shading) are plotted for (a,d) leaves and (c,f) roots. Note the different range of water potentials presented for the two species.

Fig. 2 Differences in critical embolism thresholds among species and organs of the two mangrove species and compared to previously published data for mangroves. The average (a) P_5 and (b) P50 for each organ and of *Avicennia marina* (green) and *Bruguiera gymnorrhiza* (purple). P_5 is defined as the water potential at which 5% of total embolism occurs, and P50 is defined as the water potential at 50% of total embolism. Previously reported P50 values of mature stems of mangroves based on hydraulic vulnerability curves (i.e. not optical vulnerability) are shown by grey points in (b): *Laguncularia racemosa* (Lr; Ewers *et al*., 2004), *Aegiceras corniculatum* (Ac; Jiang *et al*., 2017; Jiang *et al*., 2021b), *Rhizophora mangle* (Rm; Sperry *et al*., 1988; Melcher *et al*., 2001), *Avicennia marina* (Am; Jiang *et al*., 2017; Jiang *et al*., 2021b), *Kandelia obovata* (Ko; Jiang *et al*., 2017) and *Bruguiera gymnorrhiza* (Bg; Jiang *et al*., 2017). Note that Melcher *et al.* (2001) includes data for two populations of *Rhizophora mangle*, one coastal and one estuarine.

Fig. 3 Differences in optical vulnerability among organs within individual plants for two mangrove species. Optical vulnerability curves for each individual plant: (a-e) n = 5 seedlings of *A. marina*, and (f-i) n = 4 seedlings of *B. gymnorrhiza*. For each plant, all three organs were measured simultaneously while water potential was measured on the stem by a psychrometer or by periodic measurements of covered leaf water potential using a pressure chamber.

Fig. 4 Coordination of optical vulnerability among organs within individual plants.

Relationships between the P50 values of (a) stems and roots, (b) leaves and roots, and (c) leaves and stems of individual seedlings of *Avicennia marina* (n = 5, dark green) and *Bruguiera gymnorrhiza* (n = 4, dark purple). Each point represents the P50 value estimated from the optical vulnerability curves presented in Fig. 3. In all panels, dashed lines represent regressions across all points of both species combined, which were all significant. However, (b) only the relationship between leaf P50 and root P50 was significant within species (thick, solid lines). Significance values: *= 0.05 ** = 0.01 *** = 0.001.

Fig. 5 Hydraulic safety margins between the water potentials at which 5% of total embolism (P_5) and turgor loss (Ψ_{tlp}) occur. Colored points are for leaves and roots of *A. marina* (green) and *B. gymnorrhiza* (purple). Points represent means, and segments represent standard errors. The solid line represents the 1:1 line, where there is no safety margin.

Fig. 6 Differences in xylem anatomy among organs for two mangrove species. Vessel diameter distributions from (a,d) leaf midribs, (b,e) stems, (c,f) main roots of seedlings of (a-c) *Avicennia marina* and (d-f) *Bruguiera gymnorrhiza*. Insets show representative cross-sections of each organ of each species. Scale bars in each image are 100 μm in length.

Fig. 7 No effect of xylem anatomical traits on optical vulnerability to embolism. Relationships between (a-c) the water potential causing 5% of total embolism (P_5) or (d-f) the water potential causing 50% of total embolism (P50)and xylem anatomical traits: (a, d) thickness-to-span ratio $(t/b)^3$, (b, e) the double-wall thickness between adjacent conduits (t), and (c, f) vessel diameter (b). Organ-specific P_5 and P50 values were estimated from optical vulnerability curves presented in Fig. 4, and xylem hydraulic traits for each organ were measured from anatomical images. Each point represents the mean value in roots (n = 40-56), stem (n = 96-121), and midrib (n = 193-325), respectively, and line segments represent standard error. In (d-f), grey points represent published data for *Acer pseudoplatanus* (Losso et al., 2018), *Fagus sylvatica* (Losso et al., 2018), *Olea europaea* (Rodriguez-Dominguez et al., 2018), *Betula pubescens* (Avila et al., 2021), and sun and shade leaves and stems of *Phellodendron amurense* and *Ilex verticillata* (Avila et al., 2021).

Fig. 8 Conceptual diagram showing the hypothesized and actual order of and coordination between different drought response thresholds. Green arrows indicate increasing stomatal conductance (g_s), and blue cells indicate turgid (solid) and flaccid (shaded) cells. Graphics depict embolized conduits (orange) and functional conduits (blue) in leaves, stems, and roots. All physiological events are plotted as a function of water potential (Ψ). Mangroves were

hypothesized to be very drought tolerant with large safety margins between stomatal closure, turgor loss, and incipient embolism formation and for leaves to be more vulnerable than both roots and stems. Instead we found that these critical drought thresholds occurred over a narrow range of water potentials and that turgor loss and incipient embolism formation occurred at less negative water potentials in roots than they did in stems.

REFERENCES

Abdalla M, Ahmed MA, Cai G, Wankmüller F, Schwartz N, Litig O, Javaux M, Carminati A (2022) Stomatal closure during water deficit is controlled by below-ground hydraulics. Annals of Botany **129**:161-170

Adams HD, Zeppel MJB, Anderegg WRL, Hartmann H, Landhausser SM, Tissue DT, Huxman TE, Hudson PJ, Franz TE, Allen CD, Anderegg LDL, Barron-Gafford GA, Beerling DJ, Breshears DD, Brodribb TJ, Bugmann H, Cobb RC, Collins AD, Dickman LT, Duan H, Ewers BE, Galiano L, Galvez DA, Garcia-Forner N, Gaylord ML, Germino MJ, Gessler A, Hacke UG, Hakamada R, Hector A, Jenkins MW, Kane JM, Kolb TE, Law DJ, Lewis JD, Limousin JM, Love DM, Macalady AK, Martinez-Vilalta J, Mencuccini M, Mitchell PJ, Muss JD, O'Brien MJ, O'Grady AP, Pangle RE, Pinkard EA, Piper FI, Plaut JA, Pockman WT, Quirk J, Reinhardt K, Ripullone F, Ryan MG, Sala A, Sevanto S, Sperry JS, Vargas R, Vennetier M, Way DA, Xu C, Yepez EA, McDowell NG (2017) A multi-species synthesis of physiological mechanisms in drought-induced tree mortality. Nature Ecology & Evolution **1:** 1285-1291

Avila RT, Cardoso AA, Batz TA, Kane CN, DaMatta FM, McAdam SAM (2021) Limited plasticity in embolism resistance in response to light in leaves and stems in species with considerable vulnerability segmentation. Physiologia Plantarum **172:** 2142-2152

Ball MC (1988) Ecophysiology of mangroves. Trees **2:** 129-142

Bartlett MK, Klein T, Jansen S, Choat B, Sack L (2016) The correlations and sequence of plant stomatal, hydraulic, and wilting responses to drought. Proceedings of the National Academy of Sciences of the United States of America **113:** 13098

Bartlett, MK and Sinclair, G and Fontanesi, G and Knipfer, T and Walker, MA and McElrone, AJ (2022) Root pressure--volume curve traits capture rootstock drought tolerance. Annals of Botany **129**:389-402

Bartlett MK, Zhang Y, Kreidler N, Sun S, Ardy R, Cao K, Sack L (2014) Global analysis of plasticity in turgor loss point, a key drought tolerance trait. Ecology Letters **17:** 1580-1590

Bates D, Mächler M, Bolker B, Walker S (2014) Fitting linear mixed-effects models using lme4. Journal of Statistical Software **67:** 1-48

Bouche PS, Delzon S, Choat B, Badel E, Brodribb TJ, Burlett R, Cochard H, Charra-Vaskou K, Lavigne B, Li S (2016) Are needles of Pinus pinaster more vulnerable to xylem embolism than branches? New insights from X-ray computed tomography. Plant, cell & environment **39:** 860-870

Bourbia I, Carins-Murphy MR, Gracie A, Brodribb TJ (2020) Xylem cavitation isolates leaky flowers during water stress in pyrethrum. New Phytol **227:** 146-155

Brodersen CR, McElrone AJ, Choat B, Matthews MA, Shackel KA (2010) The dynamics of embolism repair in xylem: in vivo visualizations using high-resolution computed tomography. Plant physiology **154:** 1088-1095

Brodersen CR, Roddy AB, Wason JW, McElrone AJ (2019) Functional Status of Xylem Through Time. Annual review of plant biology **70:** 407-433

Brodribb TJ, Bienaime D, Marmottant P (2016a) Revealing catastrophic failure of leaf networks under stress. Proceedings of the National Academy of Sciences **113:** 4865-4869

Brodribb T, Carriquí M, Delzon S, McAdam S, Holbrook N (2020b) Advanced vascular function discovered in a widespread moss. Nature Plants **6:** 273-279

Brodribb TJ, Carriqui M, Delzon S, Lucani C (2017) Optical Measurement of Stem Xylem Vulnerability. Plant physiology **174:** 2054-2061

Brodribb TJ, Cochard H (2009) Hydraulic failure defines the recovery and point of death in water-stressed conifers. Plant physiology **149:** 575-584

Brodribb TJ, Holbrook NM (2005) Water stress deforms tracheids peripheral to the leaf vein of a tropical conifer. Plant Physiology **137:** 1139-1146

Brodribb TJ, Powers J, Cochard H, Choat B (2020a) Hanging by a thread? Forests and drought. Science **368:** 261-266

Brodribb TJ, Skelton RP, McAdam SA, Bienaime D, Lucani CJ, Marmottant P (2016b) Visual quantification of embolism reveals leaf vulnerability to hydraulic failure. New Phytologist **209:** 1403-1409

Cardoso AA, Batz TA, McAdam SAM (2020) Xylem embolism resistance determines leaf mortality during drought in *Persea americana*. Plant Physiology **182**: 547-554.

Charrier G, Torres-Ruiz JM, Badel E, Burlett R, Choat B, Cochard H, Delmas CEL, Domec J-C, Jansen S, King A, Lenoir N, Martin-StPaul N, Gambetta GA, Delzon S (2016) Evidence for Hydraulic Vulnerability Segmentation and Lack of Xylem Refilling under Tension. Plant Physiology **172:** 1657-1668

Choat B, Jansen S, Brodribb TJ, Cochard H, Delzon S, Bhaskar R, Bucci SJ, Feild TS, Gleason SM, Hacke UG, Jacobsen AL, Lens F, Maherali H, Martinez-Vilalta J, Mayr S, Mencuccini M, Mitchell PJ, Nardini A, Pittermann J, Pratt RB, Sperry JS, Westoby M, Wright IJ, Zanne AE (2012) Global convergence in the vulnerability of forests to drought. Nature **491:** 752-755

Clough BF (1992) Primary productivity and growth of mangrove forests. *In* R AI, A DM, eds, Tropical mangrove ecosystems, Vol 41. American Geophysical Union, Washington, DC, pp 225-249

Cochard H, Badel E, Herbette S, Delzon S, Choat B, Jansen S (2013) Methods for measuring plant vulnerability to cavitation: a critical review. Journal of Experimental Botany **64:** 4779-4791

Creek D, Lamarque LJ, Torres-Ruiz JM, Parise C, Burlett R, Tissue DT, Delzon S (2020) Xylem embolism in leaves does not occur with open stomata: evidence from direct observations using the optical visualization technique. Journal of Experimental Botany **71:** 1151-1159

Cuneo IF, Knipfer T, Brodersen CR, McElrone AJ (2016) Mechanical failure of fine root cortical cells initiates plant hydraulic decline during drought. Plant Physiology **172:** 1669-1678

Dayer S, Herrera JC, Dai Z, Burlett R, Lamarque LJ, Delzon S, Bortolami G, Cochard H, Gambetta GA (2020) The sequence and thresholds of leaf hydraulic traits underlying grapevine varietal differences in drought tolerance. Journal of Experimental Botany **71:** 4333-4344

Degraeve S, De Baerdemaeker N, Ameye M, Leroux O, Haesaert G, Steppe K (2021) Acoustic Vulnerability, Hydraulic Capacitance, and Xylem Anatomy Determine Drought Response of Small Grain Cereals. Frontiers in Plant Science **12:** 599824

Dixon HH, Joly J (1895) XII. On the ascent of sap. Philosophical Transactions of the Royal Society of London. Series B: Biological Sciences**:** 563-576

Duke NC, Kovacs JM, Griffiths AD, Preece L, Hill DJE, Oosterzee PV, Mackenzie J, Morning HS, Burrows D (2017) Large-scale dieback of mangroves in Australia's Gulf of Carpentaria: a severe ecosystem response, coincidental with an unusually extreme weather event. Marine & Freshwater Research **68:** 1816-1829

Ewers FW, Lopez-Portillo J, Angeles G, Fisher JB (2004) Hydraulic conductivity and embolism in the mangrove tree Laguncularia racemosa. Tree Physiology **24:** 1057-1062

Froux F, Ducrey M, Dreyer E, Huc R (2005) Vulnerability to embolism differs in roots and shoots and among three Mediterranean conifers: consequences for stomatal regulation of water loss? Trees **19:** 137-144

Fuenzalida TI, Bryant CJ, Ovington LI, Yoon H-J, Oliveira RS, Sack L, Ball MC (2019) Shoot surface water uptake enables leaf hydraulic recovery in *Avicennia marina*. New Phytologist **2019:** 1504-1511

Gauthey A, Peters JMR, Carins-Murphy MR, Rodriguez-Dominguez CM, Li X, Delzon S, King A, Lopez R, Medlyn BE, Tissue DT, Brodribb TJ, Choat B (2020) Visual and hydraulic techniques produce similar estimates of cavitation resistance in woody species. New Phytol 228: 884-897

Guan XY, Pereira L, McAdam SAM, Cao KF, Jansen S (2021) No gas source, no problem: Proximity to pre-existing embolism and segmentation affect embolism spreading in angiosperm xylem by gas diffusion. Plant Cell and Environment 44: 1329-1345

Hacke UG, Sperry JS, Pockman WT, Davis SD, McCulloh KA (2001) Trends in wood density and structure are linked to prevention of xylem implosion by negative pressure. Oecologia **126:** 457-461

Hothorn T, Bretz F, Westfall P (2008) Simultaneous inference in general parametric models. Biometrical Journal: Journal of Mathematical Methods in Biosciences **50:** 346-363

Jansen S, Nardini A (2014) From systematic to ecological wood anatomy and finally plant hydraulics: are we making progress in understanding xylem evolution? New Phytologist **203:** 12-15

Jiang GF, Brodribb TJ, Roddy AB, Lei JY, Si HT, Pahadi P, Zhang YJ, Cao KF (2021a) Contrasting water use, stomatal regulation, embolism resistance, and drought responses of two co-occurring mangroves. Water 13:1945.

Jiang GF, Goodale UM, Liu YY, Hao GY, Cao KF (2017) Salt management strategy defines the stem and leaf hydraulic characteristics of six mangrove tree species. Tree Physiology **37:** 389-401.

Jiang X, Choat B, Zhang Y-J, Guan X-Y, Shi W, Cao K-F (2021b) Variation in xylem hydraulic structure and function of two mangrove species across a latitudinal gradient in Eastern Australia. Water 13:850.

Johnson DM, Wortemann R, McCulloh KA, Jordan-Meille L, Ward E, Warren JM, Palmroth S, Domec J-C (2016) A test of the hydraulic vulnerability segmentation hypothesis in angiosperm and conifer tree species. Tree physiology **36:** 983-993

Johnson KM, Jordan GJ, Brodribb TJ (2018) Wheat leaves embolized by water stress do not recover function upon rewatering. Plant, cell & environment **41:** 2704-2714

Johnson KM, Brodersen C, Carins-Murphy MR, Choat B, Brodribb TJ (2020) Xylem Embolism Spreads by Single-Conduit Events in Three Dry Forest Angiosperm Stems. Plant Physiol **184:** 212-222

Jones H, Sutherland R (1991) Stomatal control of xylem embolism. Plant, Cell & Environment **14:** 607-612

Kaack L, Altaner CM, Carmesin C, Diaz A, Holler M, Kranz C, Neusser G, Odstrcil M, Schenk HJ, Schmidt V, Weber M, Ya Z, Jansen S (2019) Function and three-dimensional structure of intervessel pit membranes in angiosperms: a review. Iawa Journal 40: 673-702

Kaack L, Weber M, Isasa E, Karimi Z, Li S, Pereira L, Trabi CL, Zhang Y, Schenk HJ, Schuldt B, Schmidt V, Jansen S (2021) Pore constrictions in intervessel pit membranes provide a mechanistic explanation for xylem embolism resistance in angiosperms. New Phytologist **230:** 1829-1843

Klepsch M, Zhang Y, Kotowska MM, Lamarque LJ, Nolf M, Schuldt B, Torres-Ruiz JM, Qin DW, Choat B, Delzon S (2018) Is xylem of angiosperm leaves less resistant to embolism than branches? Insights from microCT, hydraulics, and anatomy. Journal of Experimental Botany **69:** 5611-5623

Krauss KW, Lovelock CE, Mckee KL, Lopez-Hoffman L, Ewe SML, Sousa WP (2008) Environmental drivers in mangrove establishment and early development: A review. Aquatic Botany **89:** 105-127

Krishnamurthy P, JYOTHI-PRAKASH PA, Qin L, He J, Lin Q, LOH CS, Kumar PP (2014) Role of root hydrophobic barriers in salt exclusion of a mangrove plant *Avicennia officinalis*. Plant, Cell & Environment **37:** 1656-1671

Lagomasino D, Fatoyinbo T, Castañeda-Moya E, Cook BD, Montesano PM, Neigh CSR, Corp LA, Ott LE, Chavez S, Morton DC (2021) Storm surge and ponding explain mangrove dieback in southwest Florida following Hurricane Irma. Nature Communications 12: 4003

Lens F, Sperry JS, Christman MA, Choat B, Rabaey D, Jansen S (2011) Testing hypotheses that link wood anatomy to cavitation resistance and hydraulic conductivity in the genus Acer. New phytologist **190:** 709-723

Liu H, Gleason SM, Hao G, Hua L, He P, Goldstein G, Ye Q (2019) Hydraulic traits are coordinated with maximum plant height at the global scale. Sci Adv **5:** eaav1332

Loepfe L, Martinez-Vilalta J, Pinol J, Mencuccini M (2007) The relevance of xylem network structure for plant hydraulic efficiency and safety. J Theor Biol 247: 788-803

Losso A, Bär A, Dämon B, Dullin C, Ganthaler A, Petruzzellis F, Savi T, Tromba G, Nardini A, Mayr S, Beikircher B (2018) Insights from in vivo micro-CT analysis: testing the hydraulic vulnerability segmentation in *Acer pseudoplatanus* and *Fagus sylvatica* seedlings. New Phytologist **2019:** 1831-1842

Mafigholami D, Mahmoudi B, Zenner EK (2017) An analysis of the relationship between drought events and mangrove changes along the northern coasts of the Persian Gulf and Oman Sea. Estuarine Coastal & Shelf Science **199:** 141-151

Martin-StPaul N, Delzon S, Cochard H (2017) Plant resistance to drought depends on timely stomatal closure. Ecology Letters **20:** 1437-1447

Meinzer FC (2002) Co-ordination of vapour and liquid phase water transport properties in plants. Plant, Cell & Environment **25:** 265-274

Melcher PJ, Goldstein G, Meinzer FC, Yount DE, Jones TJ, Holbrook NM, Huang C (2001) Water relations of coastal and estuarine *Rhizophora mangle*: xylem pressure potential and dynamics of embolism formation and repair. Oecologia **126:** 182-192

Nguyen HT, Meir P, Wolfe J, Mencuccini M, Ball MC (2016) Plumbing the depths: extracellular water storage in specialized leaf structures and its functional expression in a three-domain pressure-volume relationship. Plant Cell & Environment **40:** 1021-1038

Nguyen HT, Meir P, Sack L, Evans JR, Oliveira RS, Ball MC (2017) Leaf water storage increases with salinity and aridity in the mangrove *Avicennia marina*: integration of leaf structure, osmotic adjustment, and access to multiple water sources. Plant Cell & Environment **40:** 1576-1591

Olson ME, Soriano D, Rosell JA, Anfodillo T, Donoghue MJ, Edwards EJ, Leon-Gomez C, Dawson T, Martinez JJC, Castorena M, Echeverria A, Espinosa CI, Fajardo A, Gazol A, Isnard S, Lima RS, Marcati CR, Mendez-Alonzo R (2018) Plant height and hydraulic vulnerability to drought and cold. Proceedings of the National Academy of Sciences of the United States of America **115:** 7551-7556

Paliyavuth C, Clough B, Patanaponpaiboon P (2004) Salt uptake and shoot water relations in mangroves. Aquatic Botany **78:** 349-360

Pereira L, Bittencourt PR, Oliveira RS, Junior MB, Barros FV, Ribeiro RV, Mazzafera P (2016) Plant pneumatics: stem air flow is related to embolism–new perspectives on methods in plant hydraulics. New Phytologist **211:** 357-370

Pigott CDP (1993) Water as a Determinant of the Distribution of Trees at the Boundary of the Mediterranean Zone. Journal of Ecology **81:** 557-566

Purnobasuki H, Suzuki M (2005) Aerenchyma tissue development and gas-pathway structure in root of *Avicennia marina* (Forsk.) Vierh. Journal of Plant Research **118:** 285-294

Reef R, Lovelock CE (2015) Regulation of water balance in mangroves. Annals of Botany **115:** 385-395

Rockwell FE, Wheeler JK, Holbrook NM (2014) Cavitation and Its discontents: opportunities for resolving current controversies. Plant Physiology **164:** 1649-1660

Roddy AB, Jiang GF, Cao K, Simonin KA, Brodersen CR (2019) Hydraulic traits are more diverse in flowers than in leaves. New Phytologist **223:** 193-203

Roddy AB, Simonin KA, McCulloh KA, Brodersen CR, Dawson TE (2018) Water relations of Calycanthus flowers: Hydraulic conductance, capacitance, and embolism resistance. Plant Cell and Environment **41:** 2250-2262

Rodriguez-Dominguez CM, Murphy MRC, Lucani C, Brodribb TJ (2018) Mapping xylem failure in disparate organs of whole plants reveals extreme resistance in olive roots. New Phytologist **218:** 1025-1035

Sack L, Pasquet-Kok J (2011) Leaf pressure-volume curve parameters. PrometheusWiki website: http://prometheuswiki. publish. csiro. au/tikiindex. php**:** accessed 1 May 2014

Saintilan N, Khan NS, Ashe E, Kelleway JJ, Rogers K, Woodroffe CD, Horton BP (2020) Thresholds of mangrove survival under rapid sea level rise. Science **368:** 1118-1121

Schenk HJ, Espino S, Goedhart CM, Nordenstahl M, Cabrera HIM, Jones CS (2008) Hydraulic integration and shrub growth form linked across continental aridity gradients. Proceedings of the National Academy of Sciences **105:** 11248-11253

Schindelin J, Arganda-Carreras I, Frise E, Kaynig V, Longair M, Pietzsch T, Preibisch S, Rueden C, Saalfeld S, Schmid B (2012) Fiji: an open-source platform for biological-image analysis. Nature methods **9:** 676

Scholander P, Hammel H, Hemmingsen E, Garey W (1962) Salt balance in mangroves. Plant Physiology **37:** 722

Scholander PF, Bradstreet ED, Hemmingsen EA, Hammel HT (1965) Sap Pressure in Vascular Plants: Negative hydrostatic pressure can be measured in plants. Science **148:** 339-346

Scholander PF, Hammel HT, Hemmingsen EA, Bradstreet ED (1964) Hydrostatic Pressure and Osmotic Potential in Leaves of Mangroves and Some other Plants. Proceedings of the National Academy of Sciences **52:** 119-125

Schreel JDM, Van de Wal BAE, Hervé-Fernandez P, Boeckx P, Steppe K (2019) Hydraulic redistribution of foliar absorbed water causes turgor-driven growth in mangrove seedlings. Plant, Cell & Environment **42:** 2437-2447

Scoffoni C, Albuquerque C, Brodersen CR, Townes SV, John GP, Cochard H, Buckley TN, McElrone AJ, Sack L (2017) Leaf vein xylem conduit diameter influences susceptibility to embolism and hydraulic decline. New Phytologist **213:** 1076-1092

Skelton RP, Anderegg LD, Diaz J, Kling MM, Papper P, Lamarque LJ, Delzon S, Dawson TE, Ackerly DD (2021) Evolutionary relationships between drought-related traits and climate shape large hydraulic safety margins in western North American oaks. Proceedings of the National Academy of Sciences **118:** e2008987118

Skelton RP, Brodribb TJ, Choat B (2017b) Casting light on xylem vulnerability in an herbaceous species reveals a lack of segmentation. New Phytologist **214:** 561-569

Skelton RP, Brodribb TJ, McAdam SA, Mitchell PJ (2017a) Gas exchange recovery following natural drought is rapid unless limited by loss of leaf hydraulic conductance: evidence from an evergreen woodland. New Phytologist **215:** 1399-1412

Skelton RP, Dawson TE, Thompson SE, Shen Y, Weitz AP, Ackerly D (2018) Low vulnerability to xylem embolism in leaves and stems of North American oaks. Plant Physiology **177:** 1066-1077

Skelton RP, Diaz J (2020) Quantifying losses of plant hydraulic function: seeing the forest, the trees and the xylem. Tree Physiology **40:** 285-289

Smith-Martin CM, Skelton RP, Johnson KM, Lucani C, Brodribb TJ (2020) Lack of vulnerability segmentation among woody species in a diverse dry sclerophyll woodland community. Functional Ecology **34:** 777-787

Sorek Y, Greenstein S, Netzer Y, Shtein I, Jansen S, Hochberg U (2021) An increase in xylem embolism resistance of grapevine leaves during the growing season is coordinated with stomatal regulation, turgor loss point and intervessel pit membranes. New Phytologist **229:** 1955-1969

Soriano D, Echeverría A, Anfodillo T, Rosell JA, Olson ME (2020) Hydraulic traits vary as the result of tip-to-base conduit widening in vascular plants. Journal of Experimental Botany 71: 4232-4242

Sperry J, Saliendra N (1994) Intra-and inter-plant variation in xylem cavitation in *Betula occidentalis*. Plant, Cell & Environment **17:** 1233-1241

Sperry JS, Tyree MT, Donnelly JR (1988) Vulnerability of xylem to embolism in a mangrove vs an inland species of *Rhizophoraceae*. Physiologia Plantarum **74:** 276-283

Thonglim A, Delzon S, Larter M, Karami O, Rahimi A, Offringa R, Keurentjes JJB, Balazadeh S, Smets E, Lens F (2021) Intervessel pit membrane thickness best explains variation in embolism resistance amongst stems of *Arabidopsis thaliana* accessions. Ann Bot **128:** 171-182

Tomlinson PB (1986) The botany of mangroves. Cambridge University Press, Cambridge Cambridgeshire ; New York

Trueba S, Pan R, Scoffoni C, John GP, Davis SD, Sack L (2019) Thresholds for leaf damage due to dehydration: declines of hydraulic function, stomatal conductance and cellular integrity precede those for photochemistry. New Phytologist **223:** 134-149

Tyree M, Hammel H (1972) The measurement of the turgor pressure and the water relations of plants by the pressure-bomb technique. Journal of experimental Botany **23:** 267-282

Tyree MT, Ewers FW (1991) The hydraulic architecture of trees and other woody plants. New Phytologist **119:** 345-360

Tyree MT, Sperry JS (1989) Vulnerability of xylem cavitation and embolism. Annual Review of Plant Physiology & Plant Molecular Biology **40:** 19-38

Tyree MT, Zimmermann MH (2013) Xylem structure and the ascent of sap. Springer Science & Business Media

Venturas MD, Pratt RB, Jacobsen AL, Castro V, Fickle JC, Hacke UG (2019) Direct comparison of four methods to construct xylem vulnerability curves: Differences among techniques are linked to vessel network characteristics. Plant, Cell & Environment **42:** 2422-2436

Waisel Y, Eshel A, Agami M (1986) Salt balance of leaves of the mangrove *Avicennia marina*. Physiologia Plantarum **67:** 67-72

Zanne AE, Sweeney K, Sharma M, Orians CM (2006) Patterns and consequences of differential vascular sectoriality in 18 temperate tree and shrub species. Functional Ecology **20:** 200-206

Zhang FP, Brodribb TJ (2017) Are flowers vulnerable to xylem cavitation during drought? Proceedings Biological Sciences **284:** 20162642

Zhang Y, Carmesin C, Kaack L, Klepsch MM, Kotowska M, Matei T, Schenk HJ, Weber M, Walther P, Schmidt V (2020) High porosity with tiny pore constrictions and unbending pathways characterize the 3D structure of intervessel pit membranes in angiosperm xylem. Plant, cell & environment **43:** 116-130

Zhang Y, Klepsch M, Jansen S (2017) Bordered pits in xylem of vesselless angiosperms and their possible misinterpretation as perforation plates. Plant Cell and Environment **40:** 2133-2146

Zhu SD, Chen YJ, Ye Q, He PC, Liu H, Li RH, Fu PL, Jiang GF, Cao KF (2018) Leaf turgor loss point is correlated with drought tolerance and leaf carbon economics traits. Tree Physiology **38:** 658-663

Zhu SD, Liu H, Xu QY, Cao KF, Ye Q (2016) Are leaves more vulnerable to cavitation than branches? Functional Ecology **30:** 1740-1744

Zimmermann MH (1978) Hydraulic architecture of some diffuse-porous trees. Canadian Journal of Botany **56:** 2286-2295

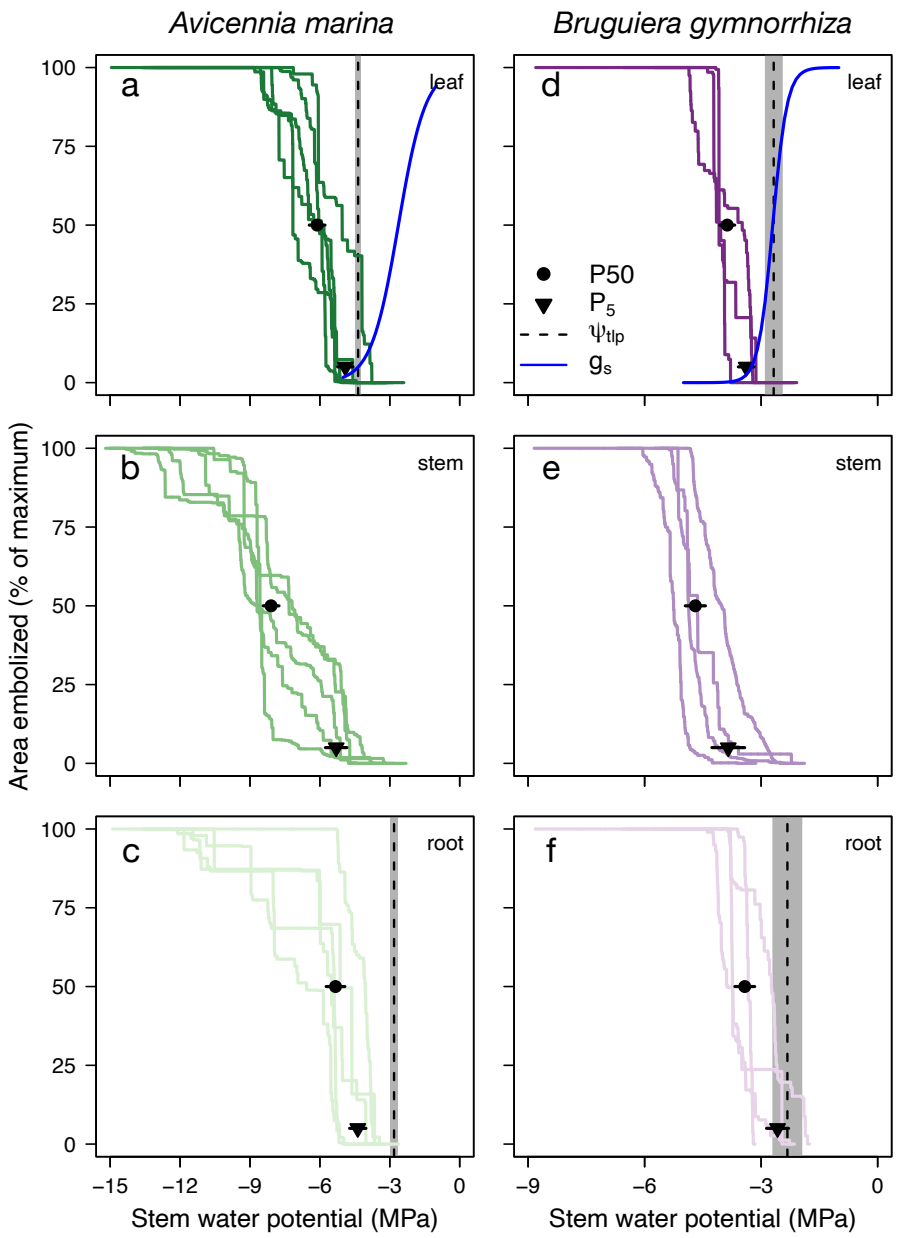

Fig. 1 The coordination between optical vulnerability, stomatal closure, and turgor loss as a function of stem water potential for two mangrove species. Optical vulnerability curves of (a) leaf, (b) stem, and (c) root of *Avicennia marina* (green lines, n = 5 seedlings), and (d) leaf, (e) stem, and (f) root of *Bruguiera gymnorrhiza* (purple lines, n = 4 seedlings). The mean water potential causing incipient (5%) of total embolism (P_5) ± s.e. (inverted black triangles and error bars) and the mean water potential causing 50% of total embolism (P50) ± s.e. (black circles and error bars) are plotted for each species x organ group. The stomatal conductance (g_s) as a function of leaf water potential for each species (blue lines; Jiang et al., 2021a) is plotted in (a)

and (d). The mean water potentials at turgor loss (Ψ_{tlp}) ± s.e. (dashed lines and grey shading) are plotted for (a,d) leaves and (c,f) roots. Note the different range of water potentials presented for the two species.

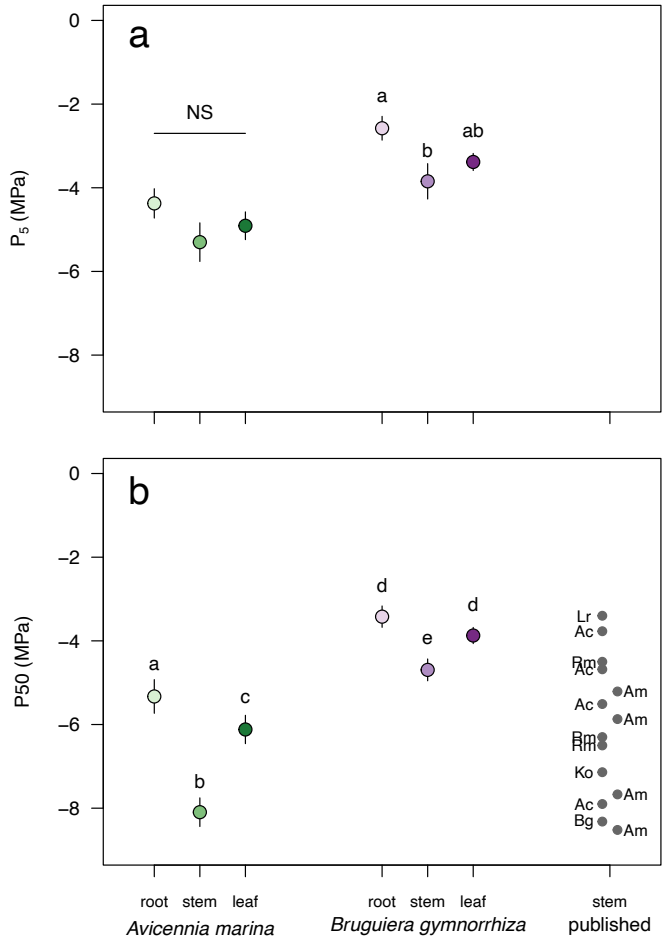

Fig. 2 Differences in critical embolism thresholds among species and organs of the two mangrove species and compared to previously published data for mangroves. The average (a) P_5 and (b) P50 for each organ and of *Avicennia marina* (green) and *Bruguiera gymnorrhiza* (purple). P_5 is defined as the water potential at which 5% of total embolism occurs, and P50 is defined as the water potential at 50% of total embolism. Previously reported P50 values of mature stems of mangroves based on hydraulic vulnerability curves (i.e. not optical vulnerability) are shown by grey points in (b): *Laguncularia racemosa* (Lr; Ewers *et al*., 2004), *Aegiceras corniculatum* (Ac; Jiang *et al*., 2017; Jiang *et al*., 2021b), *Rhizophora mangle* (Rm; Sperry *et al*., 1988; Melcher *et al*., 2001), *Avicennia marina* (Am; Jiang *et al*., 2017; Jiang *et al*., 2021b), *Kandelia obovata* (Ko; Jiang *et al*., 2017) and *Bruguiera gymnorrhiza* (Bg; Jiang *et al*., 2017). Note that Melcher *et al.* (2001) includes data for two populations of *Rhizophora mangle*, one coastal and one estuarine.

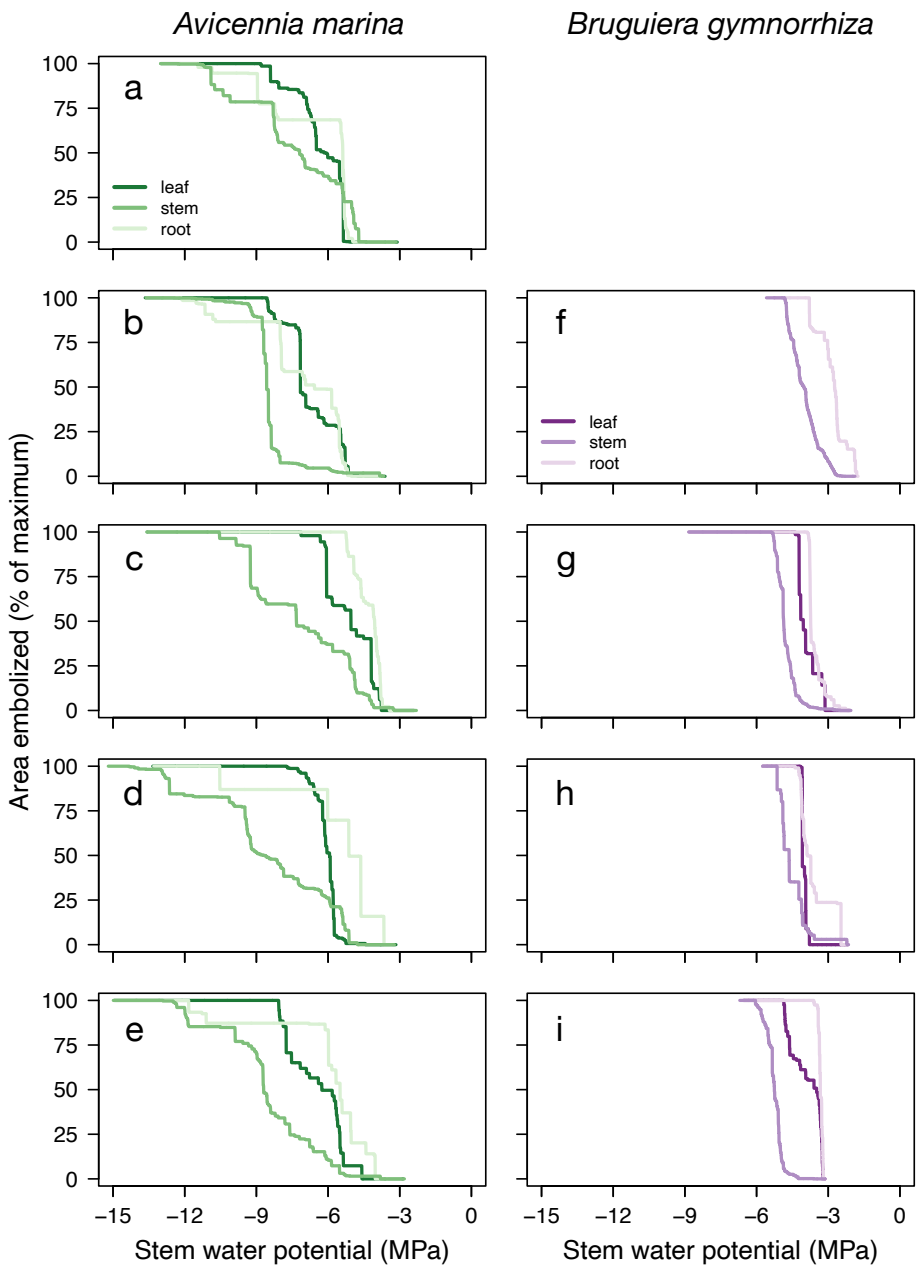

Fig. 3 Differences in optical vulnerability among organs within individual plants for two mangrove species. Optical vulnerability curves for each individual plant: (a-e) n = 5 seedlings of *A. marina*, and (f-i) n = 4 seedlings of *B. gymnorrhiza*. For each plant, all three organs were measured simultaneously while water potential was measured on the stem by a psychrometer or by periodic measurements of covered leaf water potential using a pressure chamber.

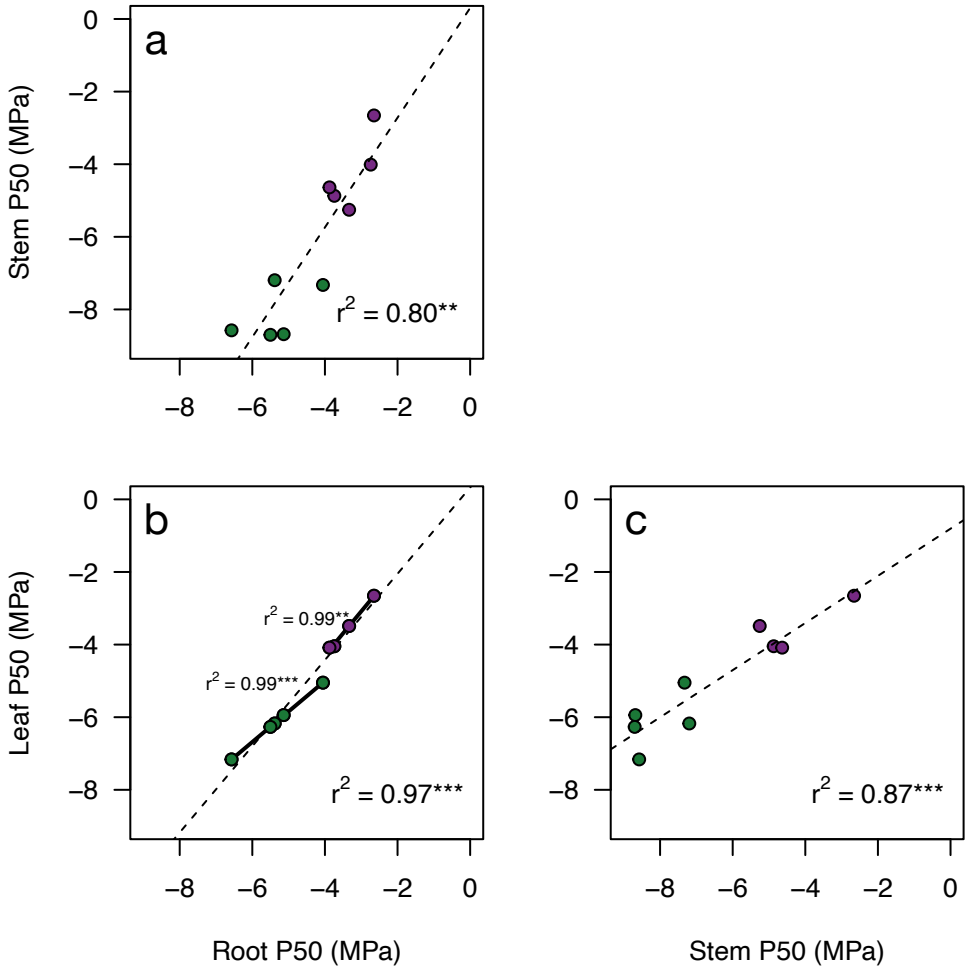

Fig. 4 Coordination of optical vulnerability among organs within individual plants. Relationships between the P50 values of (a) stems and roots, (b) leaves and roots, and (c) leaves and stems of individual seedlings of *Avicennia marina* (n = 5, dark green) and *Bruguiera gymnorrhiza* (n = 4, dark purple). Each point represents the P50 value estimated from the optical vulnerability curves presented in Fig. 3. In all panels, dashed lines represent regressions across all points of both species combined, which were all significant. However, (b) only the relationship between leaf P50 and root P50 was significant within species (thick, solid lines). Significance values: *= 0.05 ** = 0.01 *** = 0.001.

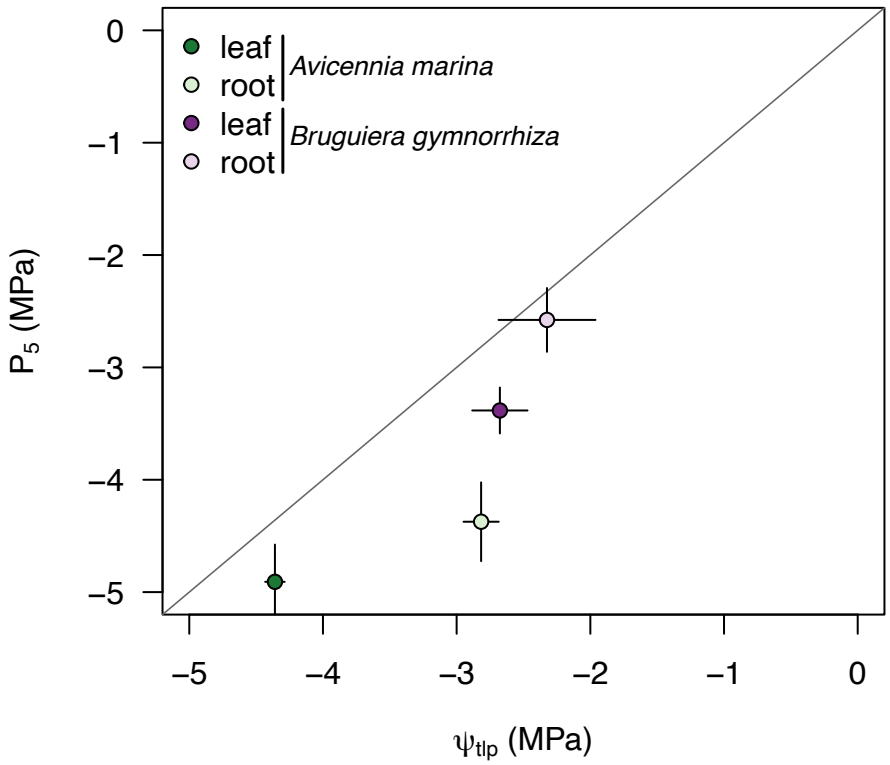

Fig. 5 Hydraulic safety margins between the water potentials at which 5% of total embolism (P_5) and turgor loss (Ψ_{tlp}) occur. Colored points are for leaves and roots of *A. marina* (green) and *B. gymnorrhiza* (purple). Points represent means, and segments represent standard errors. The solid line represents the 1:1 line, where there is no safety margin.

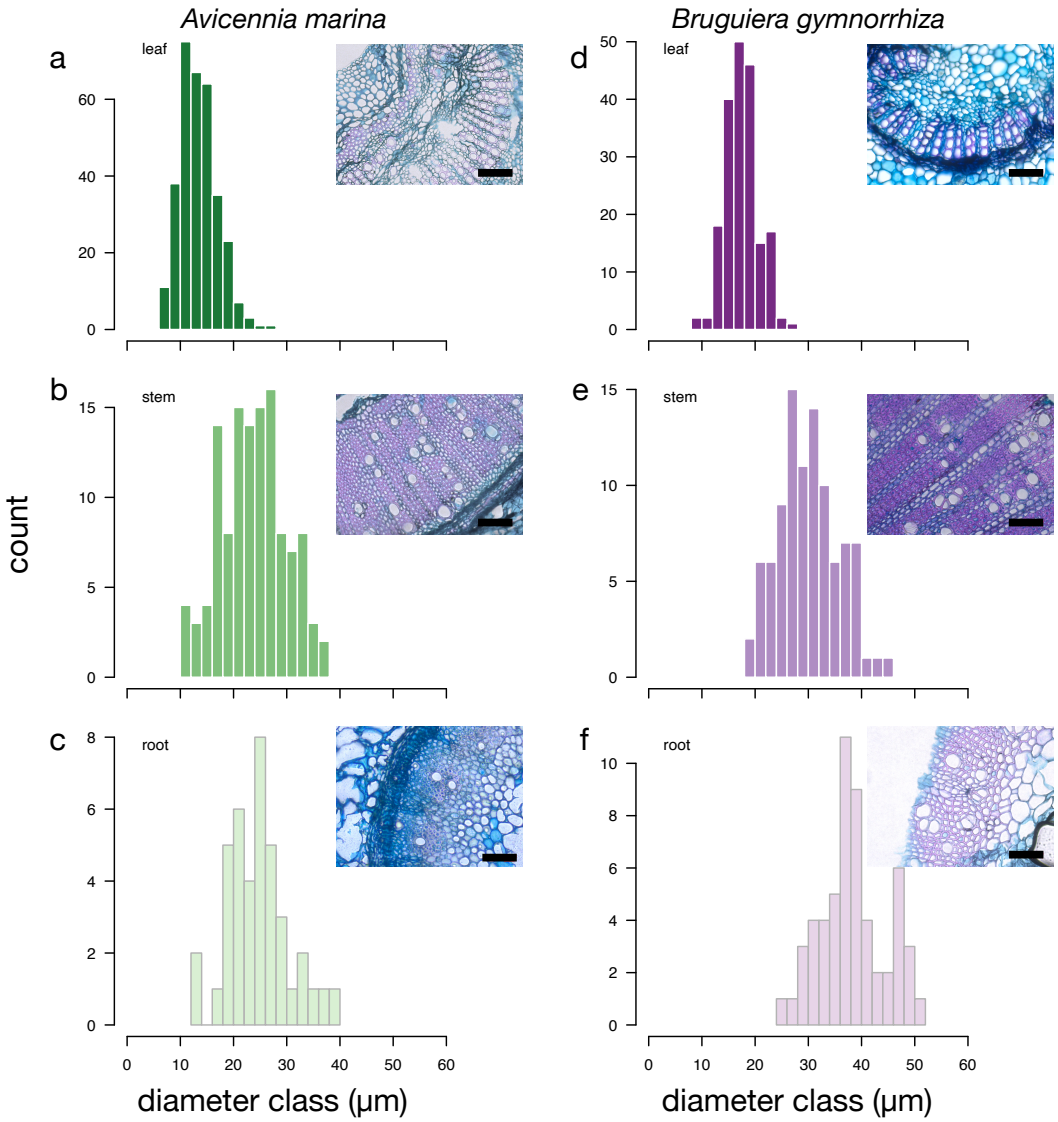

Fig. 6 Differences in xylem anatomy among organs for two mangrove species. Vessel diameter distributions from (a,d) leaf midribs, (b,e) stems, (c,f) main roots of seedlings of (a-c) *Avicennia marina* and (d-f) *Bruguiera gymnorrhiza*. Insets show representative cross-sections of each organ of each species. Scale bars in each image are 100 µm in length.

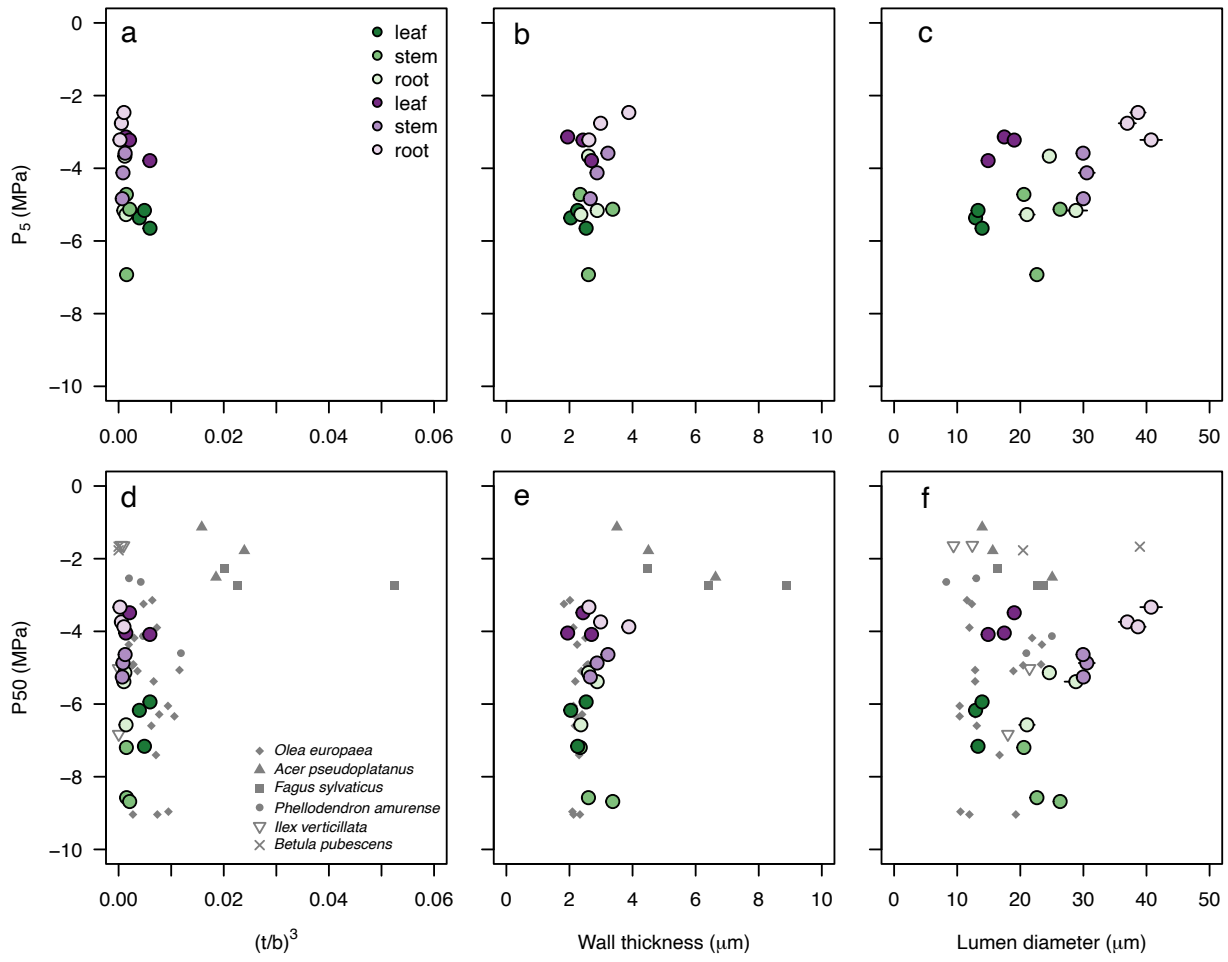

Fig. 7 No effect of xylem anatomical traits on optical vulnerability to embolism. Relationships between (a-c) the water potential causing 5% of total embolism (P_5) or (d-f) the water potential causing 50% of total embolism (P50)and xylem anatomical traits: (a, d) thickness-to-span ratio $(t/b)^3$, (b, e) the double-wall thickness between adjacent conduits (t), and (c, f) vessel diameter (b). Organ-specific P_5 and P50 values were estimated from optical vulnerability curves presented in Fig. 4, and xylem hydraulic traits for each organ were measured from anatomical images. Each point represents the mean value in roots (n = 40-56), stem (n = 96-121), and midrib (n = 193-325), respectively, and line segments represent standard error. In (d-f), grey points represent published data for *Acer pseudoplatanus* (Losso et al., 2018), *Fagus sylvatica* (Losso et al., 2018), *Olea europaea* (Rodriguez-Dominguez et al., 2018), *Betula pubescens* (Avila et al., 2021), and sun and shade leaves and stems of *Phellodendron amurense* and *Ilex verticillata* (Avila et al., 2021).

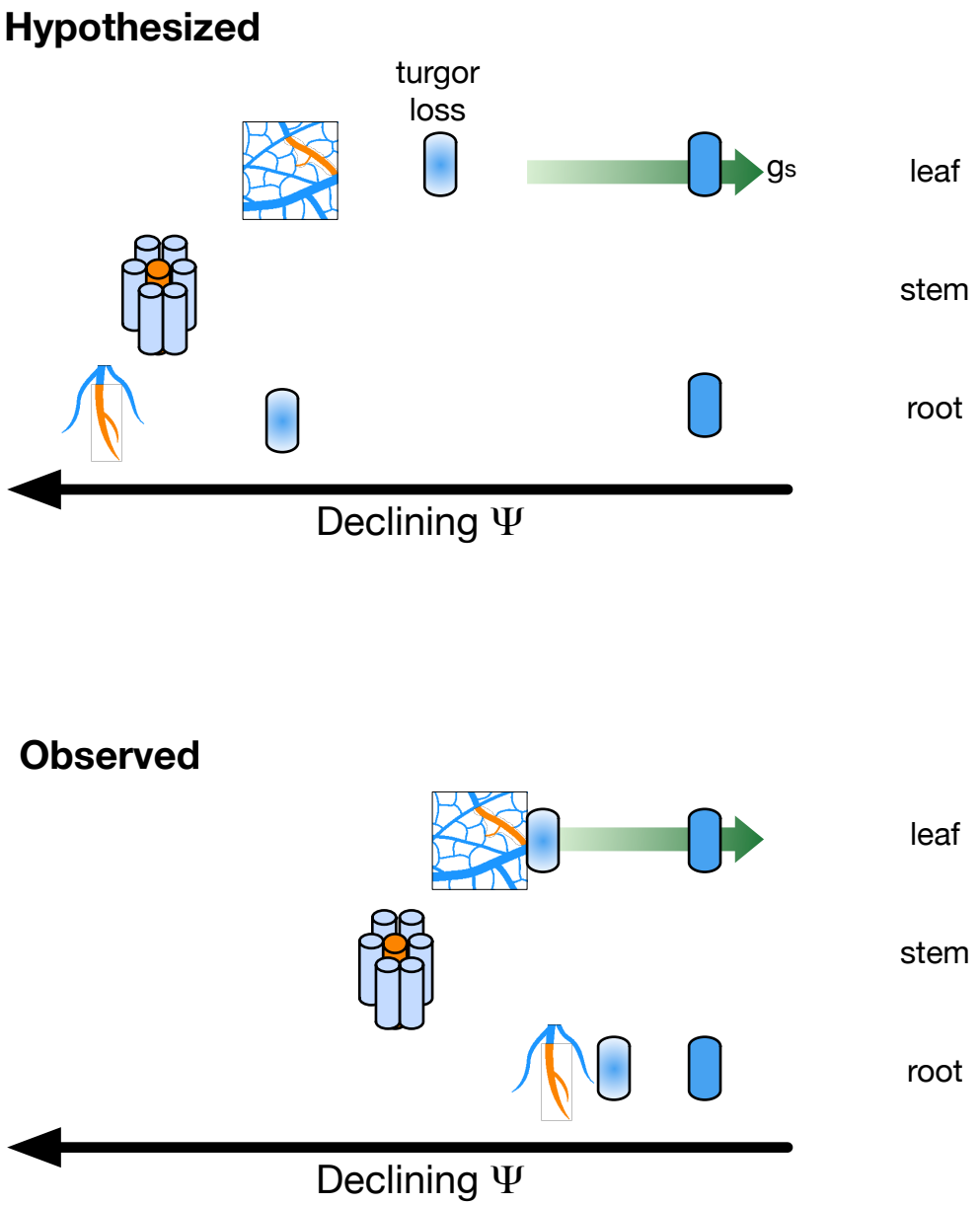

Fig. 8 Conceptual diagram showing the hypothesized and actual order of and coordination between different drought response thresholds. Green arrows indicate increasing stomatal conductance (g_s), and blue cells indicate turgid (solid) and flaccid (shaded) cells. Graphics depict embolized conduits (orange) and functional conduits (blue) in leaves, stems, and roots. All physiological events are plotted as a function of water potential (Ψ). Mangroves were hypothesized to be very drought tolerant with large safety margins between stomatal closure, turgor loss, and incipient embolism formation and for leaves to be more vulnerable than both

roots and stems. Instead we found that these critical drought thresholds occurred over a narrow range of water potentials and that turgor loss and incipient embolism formation occurred at less negative water potentials in roots than they did in stems.

Parsed Citations

Abdalla M, Ahmed MA, Cai G, Wankmüller F, Schwartz N, Litig O, Javaux M, Carminati A (2022) Stomatal closure during water deficit is controlled by below-ground hydraulics. Annals of Botany 129:161-170
Google Scholar: Author Only Title Only Author and Title

Adams HD, Zeppel MJB, Anderegg WRL, Hartmann H, Landhausser SM, Tissue DT, Huxman TE, Hudson PJ, Franz TE, Allen CD, Anderegg LDL, Barron-Gafford GA, Beerling DJ, Breshears DD, Brodribb TJ, Bugmann H, Cobb RC, Collins AD, Dickman LT, Duan H, Ewers BE, Galiano L, Galvez DA, Garcia-Forner N, Gaylord ML, Germino MJ, Gessler A, Hacke UG, Hakamada R, Hector A, Jenkins MW, Kane JM, Kolb TE, Law DJ, Lewis JD, Limousin JM, Love DM, Macalady AK, Martinez-Vilalta J, Mencuccini M, Mitchell PJ, Muss JD, O'Brien MJ, O'Grady AP, Pangle RE, Pinkard EA, Piper FI, Plaut JA, Pockman WT, Quirk J, Reinhardt K, Ripullone F, Ryan MG, Sala A, Sevanto S, Sperry JS, Vargas R, Vennetier M, Way DA, Xu C, Yepez EA, McDowell NG (2017) A multi-species synthesis of physiological mechanisms in drought-induced tree mortality. Nature Ecology & Evolution 1: 1285-1291
Google Scholar: Author Only Title Only Author and Title

Avila RT, Cardoso AA, Batz TA, Kane CN, DaMatta FM, McAdam SAM (2021) Limited plasticity in embolism resistance in response to light in leaves and stems in species with considerable vulnerability segmentation. Physiologia Plantarum 172: 2142-2152
Google Scholar: Author Only Title Only Author and Title

Ball MC (1988) Ecophysiology of mangroves. Trees 2: 129-142
Google Scholar: Author Only Title Only Author and Title

Bartlett MK, Klein T, Jansen S, Choat B, Sack L (2016) The correlations and sequence of plant stomatal, hydraulic, and wilting responses to drought. Proceedings of the National Academy of Sciences of the United States of America 113: 13098
Google Scholar: Author Only Title Only Author and Title

Bartlett, MK and Sinclair, G and Fontanesi, G and Knipfer, T and Walker, MA and McElrone, AJ (2022) Root pressure--volume curve traits capture rootstock drought tolerance. Annals of Botany 129:389-402
Google Scholar: Author Only Title Only Author and Title

Bartlett MK, Zhang Y, Kreidler N, Sun S, Ardy R, Cao K, Sack L (2014) Global analysis of plasticity in turgor loss point, a key drought tolerance trait. Ecology Letters 17: 1580-1590
Google Scholar: Author Only Title Only Author and Title

Bates D, Mächler M, Bolker B, Walker S (2014) Fitting linear mixed-effects models using lme4. Journal of Statistical Software 67: 1-48
Google Scholar: Author Only Title Only Author and Title

Bouche PS, Delzon S, Choat B, Badel E, Brodribb TJ, Burlett R, Cochard H, Charra-Vaskou K, Lavigne B, Li S (2016) Are needles of Pinus pinaster more vulnerable to xylem embolism than branches? New insights from X-ray computed tomography. Plant, cell & environment 39: 860-870
Google Scholar: Author Only Title Only Author and Title

Bourbia I, Carins-Murphy MR, Gracie A, Brodribb TJ (2020) Xylem cavitation isolates leaky flowers during water stress in pyrethrum. New Phytol 227: 146-155
Google Scholar: Author Only Title Only Author and Title

Brodersen CR, McElrone AJ, Choat B, Matthews MA, Shackel KA (2010) The dynamics of embolism repair in xylem: in vivo visualizations using high-resolution computed tomography. Plant physiology 154: 1088-1095
Google Scholar: Author Only Title Only Author and Title

Brodersen CR, Roddy AB, Wason JW, McElrone AJ (2019) Functional Status of Xylem Through Time. Annual review of plant biology 70: 407-433
Google Scholar: Author Only Title Only Author and Title

Brodribb TJ, Bienaime D, Marmottant P (2016a) Revealing catastrophic failure of leaf networks under stress. Proceedings of the National Academy of Sciences 113: 4865-4869
Google Scholar: Author Only Title Only Author and Title

Brodribb T, Carriquí M, Delzon S, McAdam S, Holbrook N (2020b) Advanced vascular function discovered in a widespread moss. Nature Plants 6: 273-279
Google Scholar: Author Only Title Only Author and Title

Brodribb TJ, Carriqui M, Delzon S, Lucani C (2017) Optical Measurement of Stem Xylem Vulnerability. Plant physiology 174: 2054-2061
Google Scholar: Author Only Title Only Author and Title

Brodribb TJ, Cochard H (2009) Hydraulic failure defines the recovery and point of death in water-stressed conifers. Plant physiology 149: 575-584
Google Scholar: Author Only Title Only Author and Title

Brodribb TJ, Holbrook NM (2005) Water stress deforms tracheids peripheral to the leaf vein of a tropical conifer. Plant Physiology 137: 1139-1146
Google Scholar: Author Only Title Only Author and Title

Brodribb TJ, Powers J, Cochard H, Choat B (2020a) Hanging by a thread? Forests and drought. Science 368: 261-266
Google Scholar: Author Only Title Only Author and Title

Brodribb TJ, Skelton RP, McAdam SA, Bienaime D, Lucani CJ, Marmottant P (2016b) Visual quantification of embolism reveals leaf vulnerability to hydraulic failure. New Phytologist 209: 1403-1409
Google Scholar: Author Only Title Only Author and Title

Cardoso AA, Batz TA, McAdam SAM (2020) Xylem embolism resistance determines leaf mortality during drought in Persea americana. Plant Physiology 182: 547-554.
Google Scholar: Author Only Title Only Author and Title

Charrier G, Torres-Ruiz JM, Badel E, Burlett R, Choat B, Cochard H, Delmas CEL, Domec J-C, Jansen S, King A, Lenoir N, Martin-StPaul N, Gambetta GA, Delzon S (2016) Evidence for Hydraulic Vulnerability Segmentation and Lack of Xylem Refilling under Tension. Plant Physiology 172: 1657-1668
Google Scholar: Author Only Title Only Author and Title

Choat B, Jansen S, Brodribb TJ, Cochard H, Delzon S, Bhaskar R, Bucci SJ, Feild TS, Gleason SM, Hacke UG, Jacobsen AL, Lens F, Maherali H, Martinez-Vilalta J, Mayr S, Mencuccini M, Mitchell PJ, Nardini A, Pittermann J, Pratt RB, Sperry JS, Westoby M, Wright IJ, Zanne AE (2012) Global convergence in the vulnerability of forests to drought. Nature 491: 752-755
Google Scholar: Author Only Title Only Author and Title

Clough BF (1992) Primary productivity and growth of mangrove forests. In R AI, A DM, eds, Tropical mangrove ecosystems, Vol 41. American Geophysical Union, Washington, DC, pp 225-249
Google Scholar: Author Only Title Only Author and Title

Cochard H, Badel E, Herbette S, Delzon S, Choat B, Jansen S (2013) Methods for measuring plant vulnerability to cavitation: a critical review. Journal of Experimental Botany 64: 4779-4791
Google Scholar: Author Only Title Only Author and Title

Creek D, Lamarque LJ, Torres-Ruiz JM, Parise C, Burlett R, Tissue DT, Delzon S (2020) Xylem embolism in leaves does not occur with open stomata: evidence from direct observations using the optical visualization technique. Journal of Experimental Botany 71: 1151-1159
Google Scholar: Author Only Title Only Author and Title

Cuneo IF, Knipfer T, Brodersen CR, McElrone AJ (2016) Mechanical failure of fine root cortical cells initiates plant hydraulic decline during drought. Plant Physiology 172: 1669-1678
Google Scholar: Author Only Title Only Author and Title

Dayer S, Herrera JC, Dai Z, Burlett R, Lamarque LJ, Delzon S, Bortolami G, Cochard H, Gambetta GA (2020) The sequence and thresholds of leaf hydraulic traits underlying grapevine varietal differences in drought tolerance. Journal of Experimental Botany 71: 4333-4344
Google Scholar: Author Only Title Only Author and Title

Degraeve S, De Baerdemaeker N, Ameye M, Leroux O, Haesaert G, Steppe K (2021) Acoustic Vulnerability, Hydraulic Capacitance, and Xylem Anatomy Determine Drought Response of Small Grain Cereals. Frontiers in Plant Science 12: 599824
Google Scholar: Author Only Title Only Author and Title

Dixon HH, Joly J (1895) XII. On the ascent of sap. Philosophical Transactions of the Royal Society of London. Series B: Biological Sciences: 563-576
Google Scholar: Author Only Title Only Author and Title

Duke NC, Kovacs JM, Griffiths AD, Preece L, Hill DJE, Oosterzee PV, Mackenzie J, Morning HS, Burrows D (2017) Large-scale dieback of mangroves in Australia's Gulf of Carpentaria: a severe ecosystem response, coincidental with an unusually extreme weather event. Marine & Freshwater Research 68: 1816-1829
Google Scholar: Author Only Title Only Author and Title

Ewers FW, Lopez-Portillo J, Angeles G, Fisher JB (2004) Hydraulic conductivity and embolism in the mangrove tree Laguncularia racemosa. Tree Physiology 24: 1057-1062
Google Scholar: Author Only Title Only Author and Title

Froux F, Ducrey M, Dreyer E, Huc R (2005) Vulnerability to embolism differs in roots and shoots and among three Mediterranean conifers: consequences for stomatal regulation of water loss? Trees 19: 137-144
Google Scholar: Author Only Title Only Author and Title

Fuenzalida TI, Bryant CJ, Ovington LI, Yoon H-J, Oliveira RS, Sack L, Ball MC (2019) Shoot surface water uptake enables leaf hydraulic recovery in Avicennia marina. New Phytologist 2019: 1504-1511

Google Scholar: Author Only Title Only Author and Title

Gauthey A, Peters JMR, Carins-Murphy MR, Rodriguez-Dominguez CM, Li X, Delzon S, King A, Lopez R, Medlyn BE, Tissue DT, Brodribb TJ, Choat B (2020) Visual and hydraulic techniques produce similar estimates of cavitation resistance in woody species. New Phytol 228: 884-897
Google Scholar: Author Only Title Only Author and Title

Guan XY, Pereira L, McAdam SAM, Cao KF, Jansen S (2021) No gas source, no problem: Proximity to pre-existing embolism and segmentation affect embolism spreading in angiosperm xylem by gas diffusion. Plant Cell and Environment 44: 1329-1345
Google Scholar: Author Only Title Only Author and Title

Hacke UG, Sperry JS, Pockman WT, Davis SD, McCulloh KA (2001) Trends in wood density and structure are linked to prevention of xylem implosion by negative pressure. Oecologia 126: 457-461
Google Scholar: Author Only Title Only Author and Title

Hothorn T, Bretz F, Westfall P (2008) Simultaneous inference in general parametric models. Biometrical Journal: Journal of Mathematical Methods in Biosciences 50: 346-363
Google Scholar: Author Only Title Only Author and Title

Jansen S, Nardini A (2014) From systematic to ecological wood anatomy and finally plant hydraulics: are we making progress in understanding xylem evolution? New Phytologist 203: 12-15
Google Scholar: Author Only Title Only Author and Title

Jiang GF, Brodribb TJ, Roddy AB, Lei JY, Si HT, Pahadi P, Zhang YJ, Cao KF (2021a) Contrasting water use, stomatal regulation, embolism resistance, and drought responses of two co-occurring mangroves. Water 13:1945.
Google Scholar: Author Only Title Only Author and Title

Jiang GF, Goodale UM, Liu YY, Hao GY, Cao KF (2017) Salt management strategy defines the stem and leaf hydraulic characteristics of six mangrove tree species. Tree Physiology 37: 389-401.
Google Scholar: Author Only Title Only Author and Title

Jiang X, Choat B, Zhang Y-J, Guan X-Y, Shi W, Cao K-F (2021b) Variation in xylem hydraulic structure and function of two mangrove species across a latitudinal gradient in Eastern Australia. Water 13:850.
Google Scholar: Author Only Title Only Author and Title

Johnson DM, Wortemann R, McCulloh KA, Jordan-Meille L, Ward E, Warren JM, Palmroth S, Domec J-C (2016) A test of the hydraulic vulnerability segmentation hypothesis in angiosperm and conifer tree species. Tree physiology 36: 983-993
Google Scholar: Author Only Title Only Author and Title

Johnson KM, Jordan GJ, Brodribb TJ (2018) Wheat leaves embolized by water stress do not recover function upon rewatering. Plant, cell & environment 41: 2704-2714
Google Scholar: Author Only Title Only Author and Title

Johnson KM, Brodersen C, Carins-Murphy MR, Choat B, Brodribb TJ (2020) Xylem Embolism Spreads by Single-Conduit Events in Three Dry Forest Angiosperm Stems. Plant Physiol 184: 212-222
Google Scholar: Author Only Title Only Author and Title

Jones H, Sutherland R (1991) Stomatal control of xylem embolism. Plant, Cell & Environment 14: 607-612
Google Scholar: Author Only Title Only Author and Title

Kaack L, Altaner CM, Carmesin C, Diaz A, Holler M, Kranz C, Neusser G, Odstrcil M, Schenk HJ, Schmidt V, Weber M, Ya Z, Jansen S (2019) Function and three-dimensional structure of intervessel pit membranes in angiosperms: a review. Iawa Journal 40: 673-702
Google Scholar: Author Only Title Only Author and Title

Kaack L, Weber M, Isasa E, Karimi Z, Li S, Pereira L, Trabi CL, Zhang Y, Schenk HJ, Schuldt B, Schmidt V, Jansen S (2021) Pore constrictions in intervessel pit membranes provide a mechanistic explanation for xylem embolism resistance in angiosperms. New Phytologist 230: 1829-1843
Google Scholar: Author Only Title Only Author and Title

Klepsch M, Zhang Y, Kotowska MM, Lamarque LJ, Nolf M, Schuldt B, Torres-Ruiz JM, Qin DW, Choat B, Delzon S (2018) Is xylem of angiosperm leaves less resistant to embolism than branches? Insights from microCT, hydraulics, and anatomy. Journal of Experimental Botany 69: 5611-5623
Google Scholar: Author Only Title Only Author and Title

Krauss KW, Lovelock CE, Mckee KL, Lopez-Hoffman L, Ewe SML, Sousa WP (2008) Environmental drivers in mangrove establishment and early development: A review. Aquatic Botany 89: 105-127
Google Scholar: Author Only Title Only Author and Title

Krishnamurthy P, JYOTHI-PRAKASH PA, Qin L, He J, Lin Q, LOH CS, Kumar PP (2014) Role of root hydrophobic barriers in salt exclusion of a mangrove plant Avicennia officinalis. Plant, Cell & Environment 37: 1656-1671

Google Scholar: Author Only Title Only Author and Title

Lagomasino D, Fatoyinbo T, Castañeda-Moya E, Cook BD, Montesano PM, Neigh CSR, Corp LA, Ott LE, Chavez S, Morton DC (2021) Storm surge and ponding explain mangrove dieback in southwest Florida following Hurricane Irma. Nature Communications 12: 4003
Google Scholar: Author Only Title Only Author and Title

Lens F, Sperry JS, Christman MA, Choat B, Rabaey D, Jansen S (2011) Testing hypotheses that link wood anatomy to cavitation resistance and hydraulic conductivity in the genus Acer. New phytologist 190: 709-723
Google Scholar: Author Only Title Only Author and Title

Liu H, Gleason SM, Hao G, Hua L, He P, Goldstein G, Ye Q (2019) Hydraulic traits are coordinated with maximum plant height at the global scale. Sci Adv 5: eaav1332
Google Scholar: Author Only Title Only Author and Title

Loepfe L, Martinez-Vilalta J, Pinol J, Mencuccini M (2007) The relevance of xylem network structure for plant hydraulic efficiency and safety. J Theor Biol 247: 788-803
Google Scholar: Author Only Title Only Author and Title

Losso A, Bär A, Dämon B, Dullin C, Ganthaler A, Petruzzellis F, Savi T, Tromba G, Nardini A, Mayr S, Beikircher B (2018) Insights from in vivo micro-CT analysis: testing the hydraulic vulnerability segmentation in Acer pseudoplatanus and Fagus sylvatica seedlings. New Phytologist 2019: 1831-1842
Google Scholar: Author Only Title Only Author and Title

Mafigholami D, Mahmoudi B, Zenner EK (2017) An analysis of the relationship between drought events and mangrove changes along the northern coasts of the Persian Gulf and Oman Sea. Estuarine Coastal & Shelf Science 199: 141-151
Google Scholar: Author Only Title Only Author and Title

Martin-StPaul N, Delzon S, Cochard H (2017) Plant resistance to drought depends on timely stomatal closure. Ecology Letters 20: 1437-1447
Google Scholar: Author Only Title Only Author and Title

Meinzer FC (2002) Co-ordination of vapour and liquid phase water transport properties in plants. Plant, Cell & Environment 25: 265-274
Google Scholar: Author Only Title Only Author and Title

Melcher PJ, Goldstein G, Meinzer FC, Yount DE, Jones TJ, Holbrook NM, Huang C (2001) Water relations of coastal and estuarine Rhizophora mangle: xylem pressure potential and dynamics of embolism formation and repair. Oecologia 126: 182-192
Google Scholar: Author Only Title Only Author and Title

Nguyen HT, Meir P, Wolfe J, Mencuccini M, Ball MC (2016) Plumbing the depths: extracellular water storage in specialized leaf structures and its functional expression in a three-domain pressure-volume relationship. Plant Cell & Environment 40: 1021-1038
Google Scholar: Author Only Title Only Author and Title

Nguyen HT, Meir P, Sack L, Evans JR, Oliveira RS, Ball MC (2017) Leaf water storage increases with salinity and aridity in the mangrove Avicennia marina: integration of leaf structure, osmotic adjustment, and access to multiple water sources. Plant Cell & Environment 40: 1576-1591
Google Scholar: Author Only Title Only Author and Title

Olson ME, Soriano D, Rosell JA, Anfodillo T, Donoghue MJ, Edwards EJ, Leon-Gomez C, Dawson T, Martinez JJC, Castorena M, Echeverria A, Espinosa CI, Fajardo A, Gazol A, Isnard S, Lima RS, Marcati CR, Mendez-Alonzo R (2018) Plant height and hydraulic vulnerability to drought and cold. Proceedings of the National Academy of Sciences of the United States of America 115: 7551-7556
Google Scholar: Author Only Title Only Author and Title

Paliyavuth C, Clough B, Patanaponpaiboon P (2004) Salt uptake and shoot water relations in mangroves. Aquatic Botany 78: 349-360
Google Scholar: Author Only Title Only Author and Title

Pereira L, Bittencourt PR, Oliveira RS, Junior MB, Barros FV, Ribeiro RV, Mazzafera P (2016) Plant pneumatics: stem air flow is related to embolism–new perspectives on methods in plant hydraulics. New Phytologist 211: 357-370
Google Scholar: Author Only Title Only Author and Title

Pigott CDP (1993) Water as a Determinant of the Distribution of Trees at the Boundary of the Mediterranean Zone. Journal of Ecology 81: 557-566
Google Scholar: Author Only Title Only Author and Title

Purnobasuki H, Suzuki M (2005) Aerenchyma tissue development and gas-pathway structure in root of Avicennia marina (Forsk.) Vierh. Journal of Plant Research 118: 285-294
Google Scholar: Author Only Title Only Author and Title

Reef R, Lovelock CE (2015) Regulation of water balance in mangroves. Annals of Botany 115: 385-395
Google Scholar: Author Only Title Only Author and Title

Rockwell FE, Wheeler JK, Holbrook NM (2014) Cavitation and Its discontents: opportunities for resolving current controversies. Plant Physiology 164: 1649-1660
Google Scholar: Author Only Title Only Author and Title

Roddy AB, Jiang GF, Cao K, Simonin KA, Brodersen CR (2019) Hydraulic traits are more diverse in flowers than in leaves. New Phytologist 223: 193-203
Google Scholar: Author Only Title Only Author and Title

Roddy AB, Simonin KA, McCulloh KA, Brodersen CR, Dawson TE (2018) Water relations of Calycanthus flowers: Hydraulic conductance, capacitance, and embolism resistance. Plant Cell and Environment 41: 2250-2262
Google Scholar: Author Only Title Only Author and Title

Rodriguez-Dominguez CM, Murphy MRC, Lucani C, Brodribb TJ (2018) Mapping xylem failure in disparate organs of whole plants reveals extreme resistance in olive roots. New Phytologist 218: 1025-1035
Google Scholar: Author Only Title Only Author and Title

Sack L, Pasquet-Kok J (2011) Leaf pressure-volume curve parameters. PrometheusWiki website: http://prometheuswiki. publish. csiro. au/tikiindex. php: accessed 1 May 2014
Google Scholar: Author Only Title Only Author and Title

Saintilan N, Khan NS, Ashe E, Kelleway JJ, Rogers K, Woodroffe CD, Horton BP (2020) Thresholds of mangrove survival under rapid sea level rise. Science 368: 1118-1121
Google Scholar: Author Only Title Only Author and Title

Schenk HJ, Espino S, Goedhart CM, Nordenstahl M, Cabrera HIM, Jones CS (2008) Hydraulic integration and shrub growth form linked across continental aridity gradients. Proceedings of the National Academy of Sciences 105: 11248-11253
Google Scholar: Author Only Title Only Author and Title

Schindelin J, Arganda-Carreras I, Frise E, Kaynig V, Longair M, Pietzsch T, Preibisch S, Rueden C, Saalfeld S, Schmid B (2012) Fiji: an open-source platform for biological-image analysis. Nature methods 9: 676
Google Scholar: Author Only Title Only Author and Title

Scholander P, Hammel H, Hemmingsen E, Garey W (1962) Salt balance in mangroves. Plant Physiology 37: 722
Google Scholar: Author Only Title Only Author and Title

Scholander PF, Bradstreet ED, Hemmingsen EA, Hammel HT (1965) Sap Pressure in Vascular Plants: Negative hydrostatic pressure can be measured in plants. Science 148: 339-346
Google Scholar: Author Only Title Only Author and Title

Scholander PF, Hammel HT, Hemmingsen EA, Bradstreet ED (1964) Hydrostatic Pressure and Osmotic Potential in Leaves of Mangroves and Some other Plants. Proceedings of the National Academy of Sciences 52: 119-125
Google Scholar: Author Only Title Only Author and Title

Schreel JDM, Van de Wal BAE, Hervé-Fernandez P, Boeckx P, Steppe K (2019) Hydraulic redistribution of foliar absorbed water causes turgor-driven growth in mangrove seedlings. Plant, Cell & Environment 42: 2437-2447
Google Scholar: Author Only Title Only Author and Title

Scoffoni C, Albuquerque C, Brodersen CR, Townes SV, John GP, Cochard H, Buckley TN, McElrone AJ, Sack L (2017) Leaf vein xylem conduit diameter influences susceptibility to embolism and hydraulic decline. New Phytologist 213: 1076-1092
Google Scholar: Author Only Title Only Author and Title

Skelton RP, Anderegg LD, Diaz J, Kling MM, Papper P, Lamarque LJ, Delzon S, Dawson TE, Ackerly DD (2021) Evolutionary relationships between drought-related traits and climate shape large hydraulic safety margins in western North American oaks. Proceedings of the National Academy of Sciences 118: e2008987118
Google Scholar: Author Only Title Only Author and Title

Skelton RP, Brodribb TJ, Choat B (2017b) Casting light on xylem vulnerability in an herbaceous species reveals a lack of segmentation. New Phytologist 214: 561-569
Google Scholar: Author Only Title Only Author and Title

Skelton RP, Brodribb TJ, McAdam SA, Mitchell PJ (2017a) Gas exchange recovery following natural drought is rapid unless limited by loss of leaf hydraulic conductance: evidence from an evergreen woodland. New Phytologist 215: 1399-1412
Google Scholar: Author Only Title Only Author and Title

Skelton RP, Dawson TE, Thompson SE, Shen Y, Weitz AP, Ackerly D (2018) Low vulnerability to xylem embolism in leaves and stems of North American oaks. Plant Physiology 177: 1066-1077
Google Scholar: Author Only Title Only Author and Title

Skelton RP, Diaz J (2020) Quantifying losses of plant hydraulic function: seeing the forest, the trees and the xylem. Tree Physiology 40: 285-289
Google Scholar: Author Only Title Only Author and Title

Smith-Martin CM, Skelton RP, Johnson KM, Lucani C, Brodribb TJ (2020) Lack of vulnerability segmentation among woody species in a diverse dry sclerophyll woodland community. Functional Ecology 34: 777-787
Google Scholar: Author Only Title Only Author and Title

Sorek Y, Greenstein S, Netzer Y, Shtein I, Jansen S, Hochberg U (2021) An increase in xylem embolism resistance of grapevine leaves during the growing season is coordinated with stomatal regulation, turgor loss point and intervessel pit membranes. New Phytologist 229: 1955-1969
Google Scholar: Author Only Title Only Author and Title

Soriano D, Echeverría A, Anfodillo T, Rosell JA, Olson ME (2020) Hydraulic traits vary as the result of tip-to-base conduit widening in vascular plants. Journal of Experimental Botany 71: 4232-4242
Google Scholar: Author Only Title Only Author and Title

Sperry J, Saliendra N (1994) Intra-and inter-plant variation in xylem cavitation in Betula occidentalis. Plant, Cell & Environment 17: 1233-1241
Google Scholar: Author Only Title Only Author and Title

Sperry JS, Tyree MT, Donnelly JR (1988) Vulnerability of xylem to embolism in a mangrove vs an inland species of Rhizophoraceae. Physiologia Plantarum 74: 276-283
Google Scholar: Author Only Title Only Author and Title

Thonglim A, Delzon S, Larter M, Karami O, Rahimi A, Offringa R, Keurentjes JJB, Balazadeh S, Smets E, Lens F (2021) Intervessel pit membrane thickness best explains variation in embolism resistance amongst stems of Arabidopsis thaliana accessions. Ann Bot 128: 171-182
Google Scholar: Author Only Title Only Author and Title

Tomlinson PB (1986) The botany of mangroves. Cambridge University Press, Cambridge Cambridgeshire ; New York
Google Scholar: Author Only Title Only Author and Title

Trueba S, Pan R, Scoffoni C, John GP, Davis SD, Sack L (2019) Thresholds for leaf damage due to dehydration: declines of hydraulic function, stomatal conductance and cellular integrity precede those for photochemistry. New Phytologist 223: 134-149
Google Scholar: Author Only Title Only Author and Title

Tyree M, Hammel H (1972) The measurement of the turgor pressure and the water relations of plants by the pressure-bomb technique. Journal of experimental Botany 23: 267-282
Google Scholar: Author Only Title Only Author and Title

Tyree MT, Ewers FW (1991) The hydraulic architecture of trees and other woody plants. New Phytologist 119: 345-360
Google Scholar: Author Only Title Only Author and Title

Tyree MT, Sperry JS (1989) Vulnerability of xylem cavitation and embolism. Annual Review of Plant Physiology & Plant Molecular Biology 40: 19-38
Google Scholar: Author Only Title Only Author and Title

Tyree MT, Zimmermann MH (2013) Xylem structure and the ascent of sap. Springer Science & Business Media
Google Scholar: Author Only Title Only Author and Title

Venturas MD, Pratt RB, Jacobsen AL, Castro V, Fickle JC, Hacke UG (2019) Direct comparison of four methods to construct xylem vulnerability curves: Differences among techniques are linked to vessel network characteristics. Plant, Cell & Environment 42: 2422-2436
Google Scholar: Author Only Title Only Author and Title

Waisel Y, Eshel A, Agami M (1986) Salt balance of leaves of the mangrove Avicennia marina. Physiologia Plantarum 67: 67-72
Google Scholar: Author Only Title Only Author and Title

Zanne AE, Sweeney K, Sharma M, Orians CM (2006) Patterns and consequences of differential vascular sectoriality in 18 temperate tree and shrub species. Functional Ecology 20: 200-206
Google Scholar: Author Only Title Only Author and Title

Zhang FP, Brodribb TJ (2017) Are flowers vulnerable to xylem cavitation during drought? Proceedings Biological Sciences 284: 20162642

Zhang Y, Carmesin C, Kaack L, Klepsch MM, Kotowska M, Matei T, Schenk HJ, Weber M, Walther P, Schmidt V (2020) High porosity with tiny pore constrictions and unbending pathways characterize the 3D structure of intervessel pit membranes in angiosperm xylem. Plant, cell & environment 43: 116-130
Google Scholar: Author Only Title Only Author and Title

Zhang Y, Klepsch M, Jansen S (2017) Bordered pits in xylem of vesselless angiosperms and their possible misinterpretation as perforation plates. Plant Cell and Environment 40: 2133-2146
Google Scholar: Author Only Title Only Author and Title

Zhu SD, Chen YJ, Ye Q, He PC, Liu H, Li RH, Fu PL, Jiang GF, Cao KF (2018) Leaf turgor loss point is correlated with drought tolerance and leaf carbon economics traits. Tree Physiology 38: 658-663
Google Scholar: Author Only Title Only Author and Title

Zhu SD, Liu H, Xu QY, Cao KF, Ye Q (2016) Are leaves more vulnerable to cavitation than branches? Functional Ecology 30: 1740-1744
Google Scholar: Author Only Title Only Author and Title

Zimmermann MH (1978) Hydraulic architecture of some diffuse-porous trees. Canadian Journal of Botany 56: 2286-2295
Google Scholar: Author Only Title Only Author and Title